Adaptive traction for optimal mobility for heavy duty vehicles

Master's thesis in Mobility Engineering

MUKESH CHOUDHARY
ADITYA MAPARI

DEPARTMENT OF MECHANCIS AND MARITIME SCIENCES
CHALMERS UNIVERSITY OF TECHNOLOGY
Gothenburg, Sweden 2024
www.chalmers.se

MASTER'S THESIS IN MOBILITY ENGINEERING

Adaptive Traction for Optimal Mobility for Heavy Duty Vehicles

Mukesh Choudhary
Aditya Mapari

Department of Mechanics and Maritime Sciences
Division of Vehicle Engineering and Autonomous Systems
Chalmers University of Technology
Gothenburg, Sweden 2024

Adaptive Traction for Optimal Mobility for Heavy Duty Vehicles
Mukesh Choudhary
Aditya Mapari

Supervisor: Christian Oscarsson (Volvo GTT), Robert Hjelte Ulmehag (Volvo GTT)
Examiner: Bengt Jacobson, Vehicle Engineering and Autonomous Systems

Master's Thesis 2024
Department of Mechanics and Maritime Sciences
Division of Vehicle Engineering and Autonomous Systems
Chalmers University of Technology
SE-412 96 Gothenburg
Telephone: 46 (0)31-772 1000

Cover: A Volvo FH16 carrying a heavy duty Volvo construction equipment in a construction site with gravel road.

Typeset in LaTeX
Printed by Chalmers Reproservice
Gothenburg, Sweden 2024

Adaptive Traction for Optimal Mobility for Heavy Duty Vehicles
Mukesh Choudhary
Aditya Mapari
Department of Mechanics and Maritime Sciences
Division of Vehicle Engineering and Autonomous Systems
Chalmers University of Technology

Abstract

This thesis addresses the critical need for developing prediction-based control allocation strategies for autonomous or manually operated vehicles within low-speed application area such as construction and mining sites. A prediction horizon focused in this thesis is approximately 50 meters. In the pursuit of safe and energy-efficient control, it is essential to harness the potential of multiple traction actuators, which traditionally operate re-actively. This project seeks to optimize these systems using predictive algorithms, given that drivers often lack the knowledge required to operate them effectively. Furthermore, the timely responsiveness of actuators is of critical importance in demanding situations. The current practice involves manual control of traction actuators, such as differential locks and electronically controlled air suspension, based on drivers' real-time observations. However, this approach is often sub-optimal, as it does not fully utilize the capabilities of these systems. To address this issue, the thesis centers on automating these traction actuators, leveraging predictive road data. It assumes the availability of upcoming road data, including road profile and predicted friction data for the next 50 meters.

The primary objective is to develop an optimal control strategy that maximizes traction while ensuring adequate steering margin. To achieve this, the thesis initially delves into understanding how these actuators influence traction and steering. Subsequently, a rule-based control allocation model is developed in MATLAB and Simulink, which is then tested with a comprehensive vehicle simulation model across various test cases. The research also extends to practical implementation. The control allocation logic is transferred to real-world conditions using real-time systems, specifically the MicroAutoBox II, on a physical truck. Impressively, the developed control function provides results in almost real-time, with a response time of only approximately 1000 milliseconds. While this computational time may be considered too high for safety-critical functions in some contexts, it remains adequate for the specific function under scrutiny, which is focused on predicting the upcoming 50-meter road conditions. In conclusion, the thesis presents a comprehensive approach to enhance traction using differential locks and axle load distribution strategy. By automating traction actuators based on predictive road data and optimizing control strategies, this research contributes to realizing safer, more energy-efficient autonomous driving systems.

Keywords: Prediction based control allocation,Traction actuators, differential locks, electronically controlled air suspension, predictive road data, real-time systems, axle load distribution, optimizing control

Acknowledgements

We extend our heartfelt gratitude to Volvo Group Trucks Technology, and specifically Christian Oscarsson and Leo Laine, for affording us the invaluable opportunity to undertake our 60-credits master's thesis. Our sincere appreciation goes out to Christian Oscarsson and Robert Hjelte Ulmehag, for their unwavering support and guidance from the very outset. We are deeply thankful to Bengt Jacobson, our esteemed examiner at Chalmers University of Technology, for providing us with invaluable guidance and direction throughout our thesis journey. We would like to express our genuine thanks to Niklas Fröjd for his invaluable assistance with the VTM and simulation environment. Additionally, we wish to acknowledge our families and friends, whose unwavering support has been a constant pillar throughout our educational journey.

Mukesh Choudhary, Aditya Mapari,
Gothenburg, June 2023

List of Acronyms

Below is the list of acronyms that have been used throughout this thesis listed in alphabetical order:

ABS	Anti-lock brake system
ATOM	Adaptive traction for optimal mobility
CG	Centre of gravity
CAN	Control area network
CIOM	Cab input output module
CCIOM	Central chassis input output module
EBS	Electronic brake system
ECS	Electronically controlled suspension
ECU	Electronic control unit
EMS	Engine management system
HIL	Hardware-in-the-loop
HMIOM	Human machine interface input output module
IAL	Inter-axle differential lock
IWL	Inter-wheel differential lock
LSD	Limited slip differentials
RAS	Rear axle steering
RCIOM	Rear chassis input output module
RCP	Rapid control prototyping
RTI	Real time interface
TECU	Transmission electronic control unit
VIL	Vehicle-in-the-loop
VMCU	Vehicle master control unit
VTM	Vehicle transport model

Nomenclature

Below is the nomenclature of indices, sets, parameters, and variables that have been used throughout this thesis.

Variables

a_{req}	Acceleration request
ω_{in}	Input wheel speed
ω_{left}	Wheel speed on the left
ω_{right}	Wheel speed on the right
ω_y	Pitch velocity of the vehicle
θ	Grade angle in radian
T_{in}	Input torque
T_{req}	Torque request
T_{left}	Wheel torque on the left
T_{right}	Wheel torque on the right
F_x	Longitudinal force
$F_{x,req}$	Longitudinal force request
$F_{x,roll}$	Longitudinal Rolling resistance force
$F_{x,grade}$	Longitudinal Grade resistance force
$F_{x,drive}$	Total longitudinal force required
$F_{x,total}$	Total longitudinal force applied on the wheels
$F_{powertrain}$	Force produced by the powertrain system
$F_{x,open}$	Longitudinal force capability with open differentials
$F_{x,IAL}$	Longitudinal force capability with inter-axle differential lock
$F_{x,IWL}$	Longitudinal force capability with inter-wheel differential lock
F_{x2}	Longitudinal force on 1st driven axle
F_{x3}	Longitudinal force on 2nd driven axle
F_z	Normal force
F_{z1}	Normal load on 1st axle
F_{z2}	Normal load on 1st driven axle
F_{z3}	Normal load on 2nd driven axle
F_s	Spring force
F_d	damping force
R	Rolling radius of the wheel
m	Mass of the vehicle

v_{req}	Vehicle longitudinal velocity request
v_x	Vehicle longitudinal velocity
v_z	Vehicle vertical velocity
v_{rz}	Vertical velocity of road
$\dot{v_x}$	Vehicle acceleration
g	Gravitational constant
l_1	Length of CG from 1st axle
l_2	Length of CG from 1st driven axle
l_3	Length of CG from 2nd driven axle
dt	Time interval for prediction model

All statements are expressed in SI units and radians unless otherwise specified.

Contents

List of Figures

List of Tables

1

Introduction

1.1 Terminology Overview

In this section, definitions of terms commonly used in this report is provided.

- $A \times B$ tractor or truck configuration means that it has total A number of wheels from which B is number of driven wheels
- An *actuator setting* can be defined as the selection of actuator/s by a predictive controller to optimize traction for upcoming road profile
- *Powertrain capabilities* is defined as the maximum longitudinal force that can be developed by wheel or axle with a given engine or motor
- *Road-wheel capabilities* is defined as the maximum force that can be developed by wheel or axle with a certain vertical load and friction coefficient between tire and road
- *Traction capabilities* is defined as the maximum longitudinal force that can be developed by driven wheel or axle. It can be limited either due to powertrain capabilities or road wheel capabilities
- *Steering capabilities* is defined as the maximum lateral force that can be generated on the steering axle. It can be limited either due to steering actuator capability or by road wheel capabilities
- *An event* is defined as change in road profile (uphill, downhill, curvature) and/or low friction surface under at least one wheel.

1.2 Background

Every truck manufacturer is focusing on developing functions that will assist the driver, ensure overall safety, improve transport efficiency, and assist in advancing the autonomous sector. One such function under development is Adaptive Traction for Optimal Mobility (ATOM). ATOM function is a centralized controller which will maximize traction by control of following actuators or functions:

1. Engine torque control
2. Individual wheel brake torque control
3. Inter axle differential lock control
4. Inter wheel differential lock control
5. Axle load distribution by electronically controlled air suspension (ECS)

A trucks operational zone can vary a lot depending on its application, working terrain, and environment. Depending on its usage, trucks have different functions and actuators to improve traction such as traction control system, differential lock, axle load distribution, all-wheel drive system, anti-lock braking system, electronic stability control, etc. Differential gear or open differential is used to allow different rotational speed of driven wheels during cornering. Whereas, differential lock is a mechanical lock that forces same rotational speed of driven wheels. This assists in improving traction if one wheel is on low friction side but resists steering as wheels cannot rotate independently during cornering. Axle load distribution function can redistribute loads on each axle such as to maximize vertical load on driven axles or one driven axle as the cost of reducing steering capabilities.

1.3 Problem motivating the project

Today, the driver controls both the differential locks and axle load distribution through a switch on the dashboard. Engagement and disengagement of such features require high experience of driving on different terrains and drivers rarely have knowledge about the operational domain of such actuators. Any improper use of these actuators can damage drive-line components, excessive tire wear, and affect maneuverability. It also takes time for such actuators to change their state. For example, before engaging differential locks, the power supply to the wheels should be stopped by lifting the throttle pedal and pushing down the clutch pedal. This is because the differentials won't lock if the wheel speeds or axle speeds are not equal. Thus it is important to lock differentials before the wheel starts to slip or before encountering a slippery zone. On the other hand, traction control function includes brake torque control and engine torque control is a reactive system controlled automatically when the wheel slip occurs. If the function is active, every time the wheel starts to slip, brakes will be applied to spinning wheels and thus can lead to high brake pad wear and energy loss.

Thus, with multiple traction actuators onboard, it is important to automate and coordinate between each actuator to improve the traction, avoid overuse/damage of any actuator component, optimize energy usage, and keep margin for the lateral motion of the vehicle. An example of test cases to be solved can be low-friction roads (snow). Here, multiple functions such as traction control, axle load distribution, and differential locks can function simultaneously to improve traction and thus optimized solution should be used considering all mentioned factors. Also, road data is becoming increasingly accessible via cloud services, GPS positions, and data recorded by preceding vehicles. This presents an exciting opportunity to explore prediction-based control allocation methods aimed at ensuring continuous traction for vehicles. The core concept of this thesis revolves around the development of prediction-based control allocation strategies, assuming prior knowledge of forthcoming road data.

1.4 Envisioned solution

ATOM is envisioned to be a rule-based predictive controller that will prepare the vehicle before the start of an event. ATOM will reduce the overuse of traction actuators and will optimize the control logic and allocation to utilize its full potential in an efficient manner. The input to the ATOM function will be upcoming road profile

and predicted friction. An algorithm will calculate the overall vehicle capabilities for each actuator setting. Vehicle capabilities includes traction and steering capabilities which will also give maximum limits of longitudinal and lateral acceleration that can be achieved with certain actuator setting without wheel slip.
A vehicle mathematical model that has all the five actuator systems mentioned above will be used. The best control allocation for each test case will be decided based on simulations, followed by optimization of control logic. The results of the simulation will be validated by implementing the control logic on a real vehicle (6 x 4 Diesel tractor). Figure 1.1 shows the envisioned solution of the problem statement

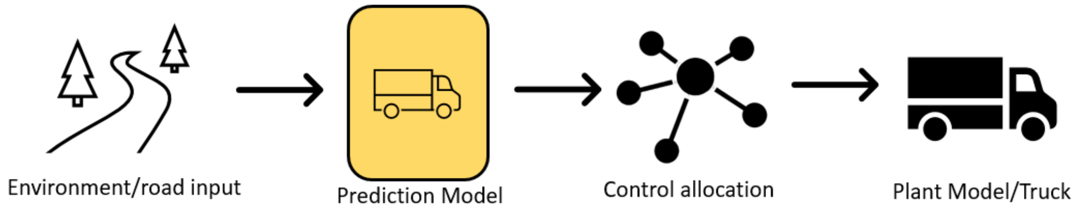

Figure 1.1: Envisioned solution

1.5 Objectives (or research questions)

The goal of the thesis is encapsulated through a set of research questions:

1. What are the conditions for engagement and disengagement of differentials?
2. Which actuator utilization is important in an event mentioned in table 3.1?
3. What is the best actuator setting based on road surface: snow, gravel, mud?
4. How to formulate algorithms to allocate actuators in different conditions?
5. How to predict and estimate the capabilities for each actuator setting?
6. How to formulate an algorithm for optimizing preferred actuator setting?
7. How ECS improve traction and what are its advantages and disadvantages?
8. How to balance lateral and traction capabilities by using ECS and differential locks?
9. How to implement the algorithm on a real vehicle?

1.6 Deliverables

- Vehicle model with ATOM function (all actuators under one centralized controller)
- Algorithm that calculates lateral and longitudinal capabilities for each actuator settings
- Predicting steering angle and yaw torque based on actuator setting
- Optimized actuator setting for each test case

- Best actuator setting for different climate conditions (snow, mud, and gravel)
- Implementation of control logic on hardware and test run on the physical truck

1.7 Limitations

- The simulations and tests are implemented for low-speed maneuvers (0 -20 kmph)
- Steady state cornering and no lateral load transfer
- Actuator delay not considered during simulations (ideal actuator differential locks)
- No TCS involved during simulations
- First order time delay used for ECS response
- No environment sensor mounted (environment assumed to be known)
- Simulations and real testing performed only with diesel trucks (no electric drive involved)
- Fixed values for desired understeer and oversteer characteristics used for each actuator settings

2

Vehicle Architecture & Actuators

This chapter provides a concise overview of vehicle architecture and the utilization of actuators for control allocation within the scope of this thesis. The exploration of vehicle architecture provides a fundamental understanding of the techniques employed in integrating systems or subsystems within the vehicle framework. This understanding serves as a foundational basis for algorithmic development aimed at effective control of the integrated components.

2.1 Vehicle Architecture:

Vehicle architecture is the arrangement and organization of components and subsystems within the vehicle, describing their interaction with each other. The architecture includes a chassis structure, powertrain, suspension and steering system, brakes assembly, electrical and electronics architecture, and other subsystems of the vehicle. The architecture of the vehicle differs according to the type of the vehicle. The focal point of this thesis is the 6x4 tractor, with specific emphasis on its suspension and powertrain actuators. The tractor features a four-point control suspension for the rear axle group. The vehicle is further equipped with a singular inter-axle differential alongside two inter-wheel differentials as shown in figure 2.1

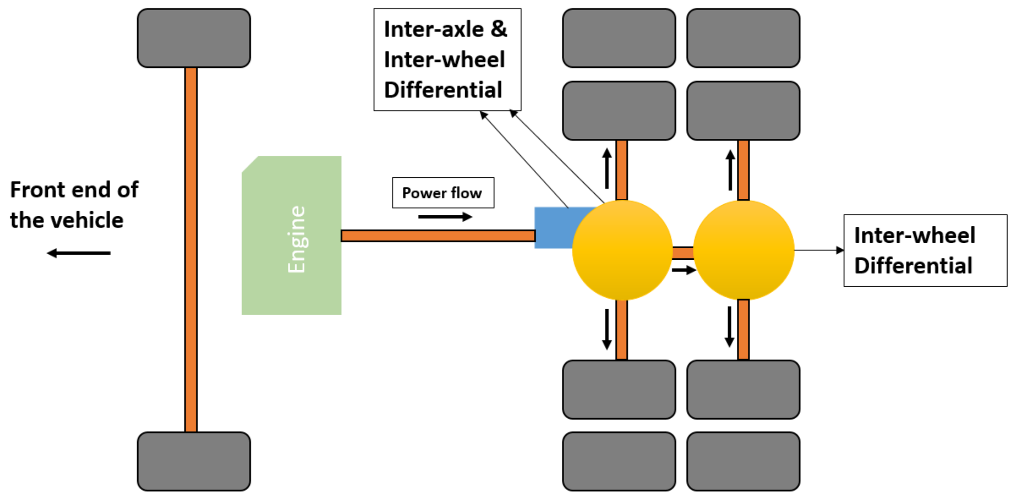

Figure 2.1: Vehicle architecture

2.2 Actuators:

Actuators serve as mechanisms transforming electrical, hydraulic, or pneumatic signals into tangible mechanical motion or force. These devices play a crucial role in vehicle manipulation, system design, and functional evolution. Control of actuators is governed by diverse Electronic Control Units (ECUs) within the vehicle's architecture.

2.2.1 Differentials:

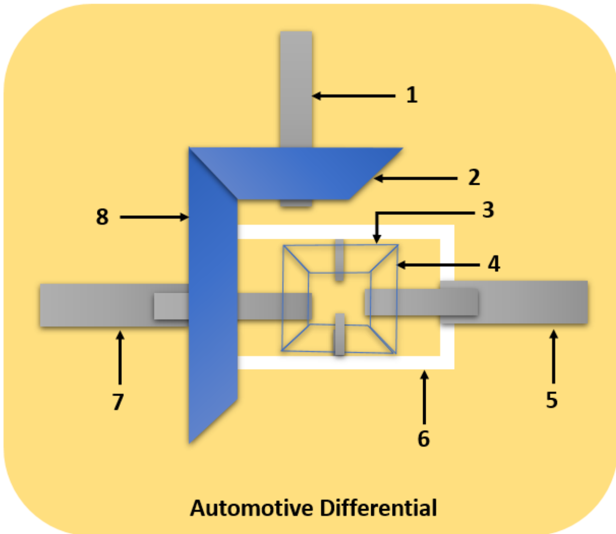

Figure 2.2: Automotive Differential with final gear

A differential is a mechanical constituent within automobiles that facilitates the transfer of torque and angular velocity from the input shaft to two distinct output shafts. The black arrows in figure 2.1 describe the power flow from the engine (including the gearbox) to the wheel. This characteristic of the differential significantly influences vehicle handling.
Figure 2.2 illustrates the mechanical configuration of an automotive differential, featuring the following components:

1. Input shaft from engine
2. Final gear pinion
3. Planet Pinion
4. Sun gear
5. To right axle shaft
6. Cage
7. To left axle shaft
8. Final gear crown wheel

While the intricate mechanics of differentials won't be covered in detail, the further sections will delve into their impact on torque distribution and wheel speeds.

2.2.2 Open differentials

The open differential is a fundamental type of differential used to transmit equal torques to wheels while allowing them to rotate at different angular speeds. When a vehicle goes around a curvature, the outside wheel has to cover longer distance than the inner wheel. And thus, outer wheel has to rotate faster than inner wheel. The open differential facilitates this difference in wheel speed by rotating planetary gears. The combined angular velocities of the output shafts are in a fixed ratio of the input shaft's angular velocity. The following equations delineate the governing principle of an open differential:

$$\omega_{in} = \frac{\omega_{left} + \omega_{right}}{2} \tag{2.1}$$

$$T_{left} = T_{right} \tag{2.2}$$

$$T_{in} = T_{left} + T_{right} \tag{2.3}$$

where, T_{in} and ω_{in} are torque and angular speed to input shaft of differential.
T_{left}, T_{right}, ω_{left}, ω_{right} are torques and angular speeds of output shaft of differential.

For a 6 x 4 tractor, the inter-axle differential splits the torque from the transmission into 50% to the first driven axle's inter-wheel differential and 50% to the second driven axle's inter-wheel differential. The torque at all driven wheels are equal and is given by:

$$T_{i,j} = \frac{T_{in}}{4} \tag{2.4}$$

where, i = 2 or 3 (driven axles), j = left or right wheel

The maximum traction force generated by a driven wheel is limited either by maximum engine power or the road wheel capabilities. The maximum road wheel capabilities for a wheel is defined as:

$$F_x = \mu_{i,j} \cdot F_{z,i,j} \tag{2.5}$$

The maximum torque transmitted by an open differential for 6 x 4 limited by the road wheel capabilities is given by:

$$T_{in} = 4 \cdot min(\mu_{ij} \cdot F_{z,ij}) \cdot r \tag{2.6}$$

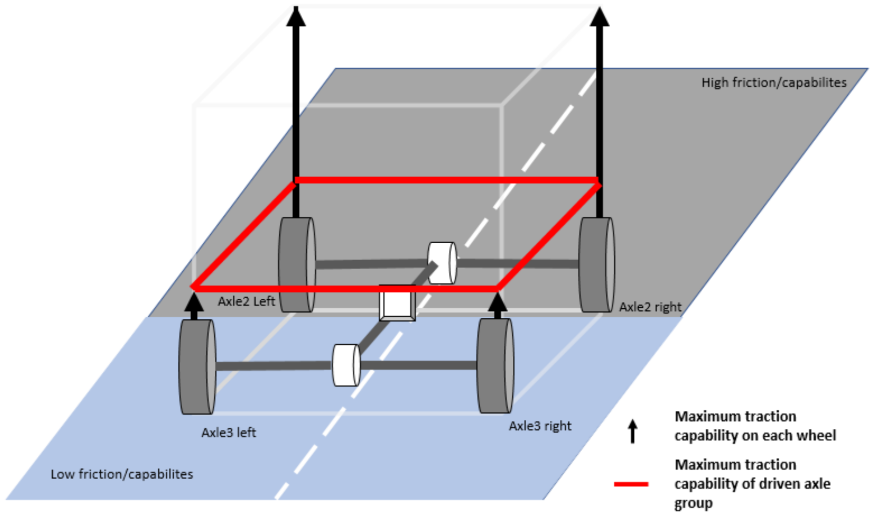

Figure 2.3: Open differential capabilities

Figure 2.3 illustrates the configuration of the driven rear axle group, featuring two inter-wheel differentials and an inter-axle differential. The axle situated at the rear is positioned on a low-friction surface, while the other axle is on high-friction terrain. The vertical black arrows indicate the maximum road wheel capabilities for each individual wheel. Since all the differentials are in an open state, the overall torque for the axle group is restricted by the rearmost axle's capabilities. The red line depicts the upper limit of the force that each wheel and the entire axle group can optimally utilize. To avoid such situations, inter-axle differentials can be locked to improve traction by using both axle's capabilities.

2.2.3 Limited slip differential

A Limited Slip Differential (LSD) is a differential variant utilized to enhance traction and handling in vehicles. It is also referred to as torque-bias or torque-proportioning differentials. These differentials function similar to open differentials when subjected to moderate drive torque. However, they can partly emulate locked differentials when slip occurs on one of the wheels. This mechanism directs torque to the wheel with superior traction, thereby enhancing overall traction capacity. This locking behavior is executed through mechanical, hydraulic, or electro-mechanical actuators. Various LSD types exist, including mechanical LSD, viscous LSD, and electro-mechanical LSD. While their modes of operation differ, the shared goal is to minimize wheel slip and augment the vehicle's traction capability. Notably, the 6x4 truck used in this thesis lacks a Limited Slip Differential, rendering it beyond the scope of this research focus.

2.2.4 Locked Differential

When any of the driven wheel is on low friction surface or has comparatively less vertical load, the wheel starts to rotate with faster speed due to open differential and thus the vehicle can get stuck. To avoid this, the inter-axle differential and inter-wheel differentials can be locked from a swtich from the dashboard. The interaxle is always locked first followed by interwheel. This is due to how the torque is transferred and mechanical connections. When any of the differential is locked, both the output shafts rotate with same angular speed. Although, in such a case, the torque transmistted to both output shafts depends upon each wheels capability. The maximum torque transmitted by locked differential limited by road wheel capabilites is given by:

$$T_{in} = \sum(\mu_{ij} \cdot F_{z,ij}) \cdot r \tag{2.7}$$

In case the inter-axle differential is locked, it transmits equal angular velocities to the first and the second inter-wheel differential input shaft. When the inter-wheel differentials are locked the left and the right wheels on the axle rotate with the same angular velocity.

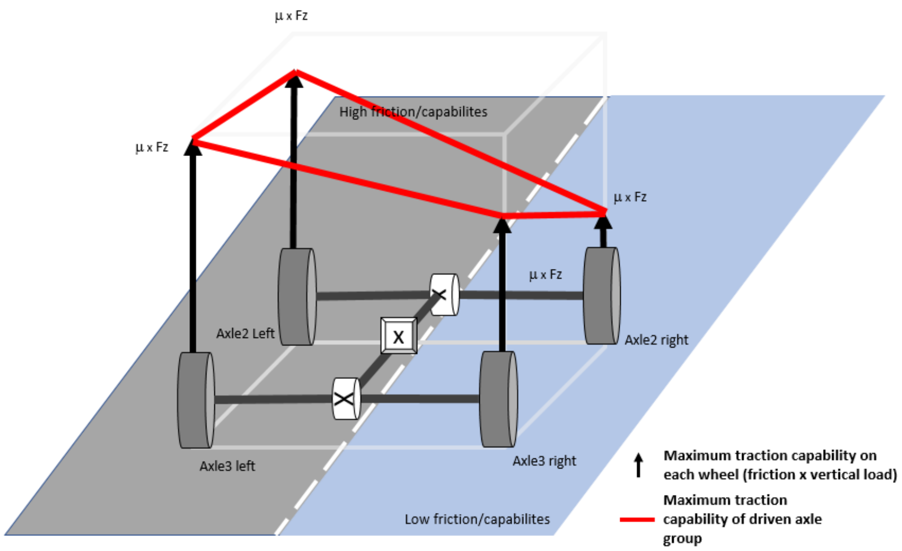

Figure 2.4: All differentials locked capabilities

In Figure 2.4, the arrangement of the driven rear axle group is depicted, which includes two inter-wheel differentials and an inter-axle differential. The wheels on the right side are situated on a low-friction surface, thus exhibit reduced road wheel capabilities, as indicated by the vertical black arrows. In such scenarios, the overall capability of the entire axle group becomes limited, whether due to the open differentials or even when the inter-axle differential is locked. To enhance traction, torque can be redirected to the left wheel by engaging the inter-wheel differentials. In the depicted figure, all the differentials are locked, allowing each wheel to utilize its maximum capability Although locking differentials provide advantages in terms of traction, it's not advisable to navigate turns with locked differentials, as both the left and right wheels should rotate freely during this maneuver. Locked differentials compel the wheels to rotate at the same speeds, generating an external yaw torque that results in vehicle understeer, as elaborated in a subsequent chapter. Additionally, if the vehicle is on surfaces with varying coefficients of friction (split mu surfaces), the torque on the left and right wheels can differ, leading to uneven longitudinal force and an additional yaw torque.

2.3 Traction control system:

Traction control is a responsive control system designed to prevent wheel spin. It employs either engine torque reduction or brake application to counteract wheel slippage. The control unit continuously monitors wheel speeds and vehicle speed through various sensors and estimation techniques. When the system detects wheel slip, it initiates a reduction in engine torque. This reduction curtails the power delivered to the driven wheels, effectively mitigating the slip. This can be achieved by adjusting throttle input, limiting fuel delivery, or employing tire models to calculate the optimal engine RPM required. Additionally, the brake control unit may intervene by applying brakes to the spinning wheel, thereby redistributing power to the other driven wheel due to the differential effect. In the context of this thesis, which focuses on predicting wheel slip, the conventional reactive control system described above is not directly employed within the developed predictive controller. However, it's worth noting that the thesis provides a solution aimed at minimizing the necessity for such reactive control measures.

2.4 Electronically controlled air suspension (ECS):

While the construction and mathematical modeling of the Electronically Controlled Suspension (ECS) are beyond the scope of this thesis and remain unspecified, its profound influence on vehicle dynamics is paramount for controller development.
In the context of a 6 x 4 vehicle configuration, the ECS system is located on the rear-driven axle, providing precise control over each driven wheel through a 4-point control mechanism. The ECS control logic predominantly encompasses three key components: sensors, an air calculation controller, and limiters. Sensors are strategically positioned on each wheel or axle to furnish essential data, including the vehicle's height and roll angle concerning the ground. The control unit leverages this data to compute load requests for each axle. These requests are generated either in response to driver input or with the goal of maintaining the chassis parallel to the ground. The limiter plays a critical role in monitoring the controller and can intervene by halting valves if necessary.
Broadly, the ECS system governs the air volume within the bellows to regulate axle loads between the two rear-driven axles. ECS operation encompasses two distinct modes: normal mode and maximum traction mode, with the driver activating these modes via a dashboard switch. In normal mode, the ECS system equalizes vertical loads on the driven wheels, ensuring uniform distribution. Conversely, in maximum traction mode, the system reallocates the loads to concentrate the maximum vertical load on a first-driven axle, thus optimizing traction.
The rearmost driven axle can be entirely lifted to enhance the load on the foremost driven axle. If the steering capabilities need to be increased or load on the front axle, the first driven axle can distribute the load to the rearmost axle but cannot be fully lifted, maintaining a minimum load of 1250 kg. Furthermore, the ECS system possesses the capability to balance load distribution between the left and

right sides, with external requests potentially altering load distribution through roll torque adjustments. However, the extent of roll torque adjustment is contingent on the current load and bellow pressure on each wheel.
Alternatively, in an 8 x 4 configuration, non-driven axles like tag or pusher axles can be raised to increase vertical loads on the driven axles. Nevertheless, it is important to note that augmenting vertical loads on the drive axle to enhance traction may result in diminished vertical load on the steering axle (front axle), thereby constraining steering capabilities.

2.5 Actuator dynamics:

To develop a controller, it's crucial to understand the behavior and response characteristics of the actuators. The ECS systems, which include pneumatics, operate relatively slowly, taking approximately 5-10 seconds to achieve vertical load or roll torque requests. In contrast, TCS systems are exceptionally fast, responding within milliseconds as soon as wheel spin is detected.
One of the most complex aspects to grasp is the dynamics of differentials, as changing their state requires every shaft to rotate at the same speed. Understanding the preconditions for differential state changes is essential before embarking on controller development.
To gain insights into this, a straightforward lock and unlock test of differentials was conducted using an electric 4x2 tractor, featuring only one inter-wheel differential and no inter-axle differential. The results of this test are presented in figure 2.5 and figure 2.6, both of which contain four distinct graphs. The x-axis in all these graphs represents time in seconds.

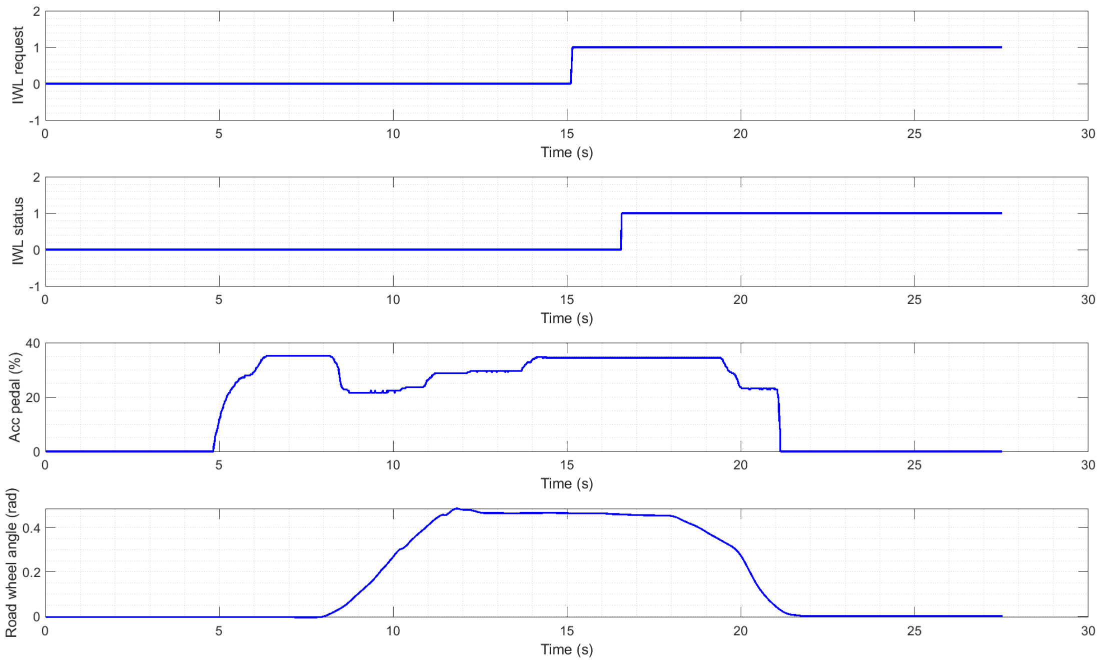

Figure 2.5: Locking of inter-wheel differential on a 4x2 tractor

Figure 2.5 illustrates the test of locking the differentials while turning. Notably, there's a delay between the driver's request for inter-wheel differential lock at 15 seconds and the actual locking of the differential at around 16.5 seconds. This delay, though expected, reveals that there is a time delay between the request and the locking action. Additionally, it was observed that the differentials are locked even when the output shafts rotate at different speeds and constant throttle requests.

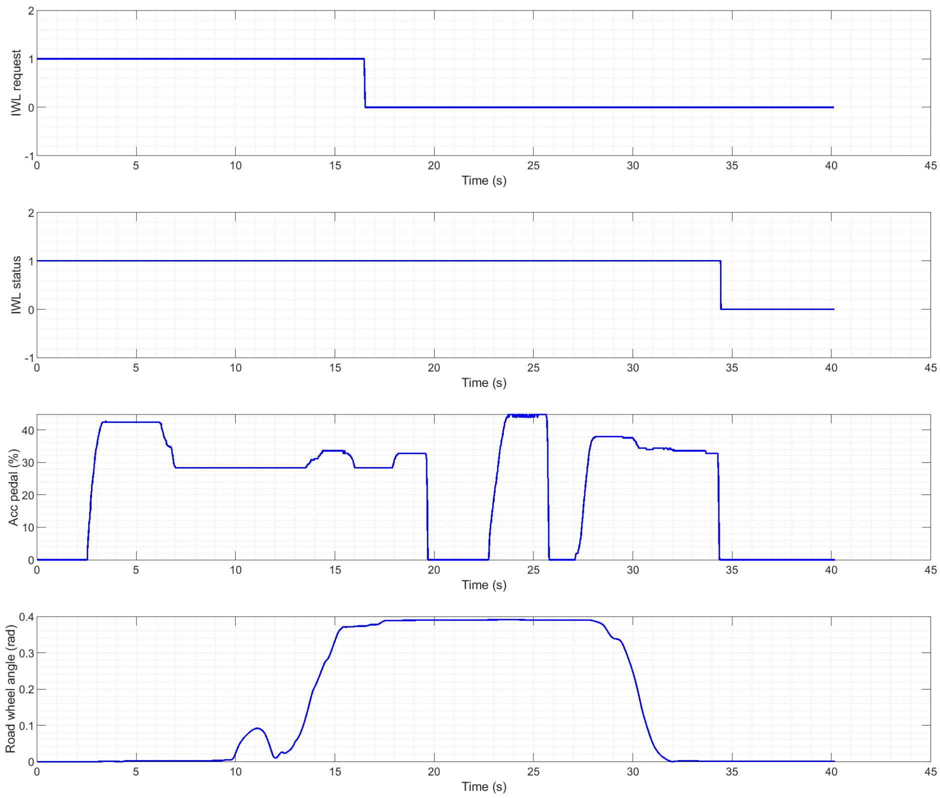

Figure 2.6: Unlocking of inter-wheel differential on a 4x2 tractor

The figure 2.6 represents the test of unlocking the differentials during a turn. This test is a continuation of the previous locking test. Here, we observe that the unlock request for the differential is initiated at around 15.1 seconds. Despite consistent throttle response and road wheel angle, the differential doesn't unlock. Various permutations were tested, such as changing the throttle response to zero and then applying throttle again, as well as setting the road wheel angle to zero while maintaining straight-line travel. None of these actions resulted in differential unlocking. Finally, at around 35 seconds, the differential unlocked in response to a request made at 15.1 seconds when both throttle request and road wheel angle are zero. This observation highlights that numerous dynamic factors influence the locking and unlocking of differentials. This is one more reason to have a prediction-based controller for such actuators so that the states can be changed before encountering an event. It's important to note that both tests were conducted at low speeds (less than 10 km/h) on a high-friction surface. Due to time constraints and limited truck availability, further tests were not conducted, which would have involved low-friction surfaces and variations in speed and turn radius.

3

Test Cases

This chapter represents explanation of test cases for traction event. The aim of the ATOM controller is to minimize wheel slips or maximize traction force in all operating conditions. Thus, below test matrix is covered in this thesis.

Traction Event	Conditions
Take off	High friction
	Low friction
	Split friction
Steep uphill	20 % grade
Uphill	Low friction Grade <16 %
	Split friction
Roundabout	Curve radius:12,20,50 meters
Uphill with turn	Low friction, Grade <10 % Curve radius: 12, 20 meters

Table 3.1: Test cases matrix

3.1 Road Surface

High mu and low friction is a road surface having same coefficient of friction under all wheels. Split mu is a road surface having different coefficient of friction under left and right wheels. Table 3.2 shows categorization of friction type and its corresponding value.

Friction type	**Example of surface**	**Coefficient of friction**
Low mu	Ice, snow, mud	0.1-0.4
Intermediate mu	Wet asphalt and concrete, gravel soft, gravel compact	0.4-0.8
High mu	Dry asphalt or concrete	0.8-1

Table 3.2: Road surface and coefficient of friction

3.2 Longitudinal test cases

Longitudinal test cases involves events where vehicle performance is evaluated only to study traction and least focus is on handling characteristics

3.2.1 Take off event

Take off event can be described as forward motion of vehicle from standstill. This event is important in trucks as it requires high amount of torque to overcome inertia. The maximum torque that can be applied to wheels is restricted by either powertrain capabilities or road wheel capabilities. To cover different scenarios that truck might come across, take off event on all three different road surface types is evaluated.

On high friction, maximum torque can be delivered to wheels without any wheel slips. On low friction and split mu, the torque is limited by road wheel capabilities and thus can introduce high wheel slip restricting the forward motion of the vehicle, increasing tire wear and fuel consumption. On soft surfaces especially on construction sites, the wheel spin can lead to increased rolling resistance as the wheels starts to sink into the ground thus restricting the forward motion of the vehicle.

3.2.2 Uphill event

Uphill gradient event is performed to evaluate gradeability. Gradeability can be defined as maximum grade that a vehicle can move forward at a constant speed with given powertrain and road wheel capabilities. As the thesis involves traction improvement, road surface used is low friction and split mu so that traction loss due to road wheel capabilities can be evaluated and optimized. Special test cases such as soft-road with uphill require knowledge about road dynamics and are not evaluated. The transition of road from straight to uphill can be smooth or step. For step transition of slope as shown in figure 3.1, the normal force on first driven axle reduces and start to spin. This happens if the uphill is around 15 to 20 %. For most of the road, transition of road is smooth. Thus there is less possibility of getting stuck due to lifting first driven axle. But as the vehicle is moving uphill, it has to overcome grade resistance. The increased torque demand can lead to wheel slip if the friction is low.

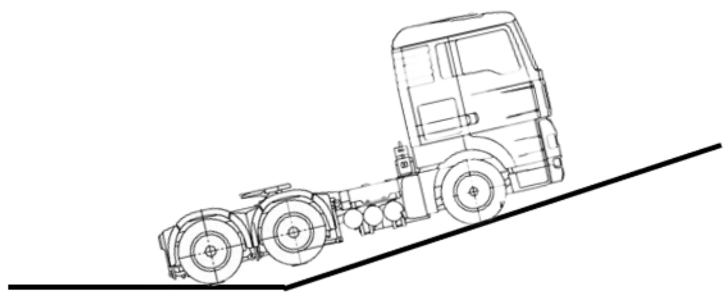

Figure 3.1: Uphill test case: Reduced vertical load on first driven axle

3.3 Combined longitudinal and lateral test cases

It involves events where vehicle performance is evaluated to study traction and handling characteristics simultaneously.

3.3.1 Roundabout or crossroad

The test case includes steady-state cornering with constant radius turn on a low friction surface. Due to weight transfer and lateral wheel/axle scrubbing, the inner wheel loses road wheel capabilities and starts to spin. Differential locks can be used to avoid inner wheel spin but it affects handling performance. Thus, it is important to improve traction with sufficient steering capabilities. Wheel/axle scrubbing and the effect of differential locks on cornering are explained in appendix A.1.

3.3.2 Uphill with turn

Uphill gradient and curvature add resistance to motion and thus require additional torque to maintain the speed. Smaller curvature adds lateral scrubbing lifting one wheel. This is a special test case where improper use of actuators can lead to vehicle instability. Thus, an optimized solution should be predicted to balance traction and steering capabilities.

4

Methodology

The schematic of the methodology is shown in the figure 4.1:

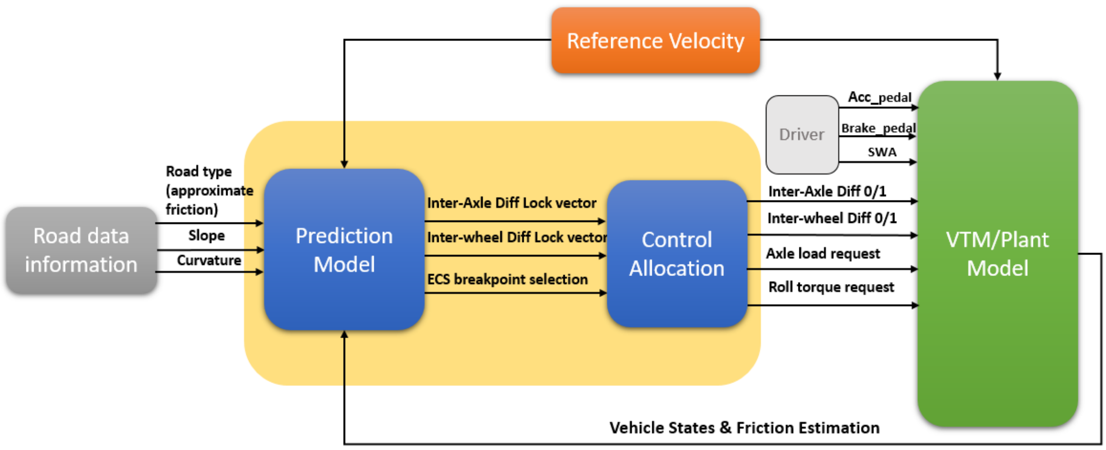

Figure 4.1: ATOM controller layout with plant model (Yellow block is developed in this thesis)

4.1 Road Data Information:

The thesis considers that the road input is available from vision based systems and cloud based map data systems. The road static attributes like slope and curvature can be obtained from cloud based map data. The dynamic road attributes like surface type can be obtained through vision based systems line camera.

4.2 Prediction Model:

The primary objective of the thesis is to calculate the maximum longitudinal and lateral capabilities of the vehicle with locked differentials. In order to understand and optimize any vehicle dynamics system it is always necessary to model the systems. Simplification of models is important to keep the analysis of the system clear. Apart from being uncomplicated the model should capture all the necessary dynamics and attributes of the system. The prediction model is a representation of the plant model/truck in the simplest possible way. The model is based on assumptions, approximations and simplifications.
In the model based approach, first a problem description/test case was formulated

for the existing tractor FH-2072. The output of the system to the problem was identified. The prediction model is designed in the following two steps:

Physical modelling:
In order to understand the problem along with analysis of the mathematical model of the vehicle, free body diagrams are necessary. The prediction model should be able to capture both longitudinal and lateral dynamics of the vehicle. For this the first step was kinetic one track modelling for longitudinal dynamics of the vehicle.
The static parameters of the vehicle like, axle loads, CG position, wheel track, powertrain specifications, inertia's, spring stiffness, damping coefficients, etc. are parameterized for the model. If the plant model changes the static parameters are also changed for the prediction model.

Kinetic one-track model:

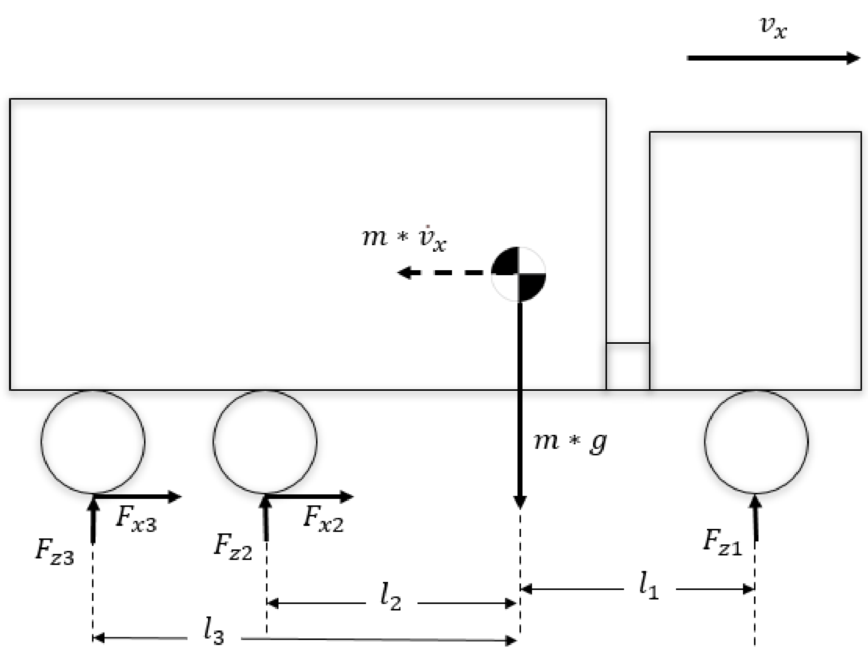

Figure 4.2: Kinetic one track model for 6x4 Truck

In order to capture the normal loads on the axles for various test cases, a simple kinetic one track model was used as shown in the figure. For test cases like, a straight road with a sharp ramp up, it was necessary to capture and analyse the variation of the normal loads on the axles. In this test case the first driven axles loses all the normal load on it for a few seconds which causes it to lose traction.

Kinetic two-track model:
The thesis involves locking of differentials. having open differential, the torque is transmitted equally to all the driven wheels. But by locking the differentials the torque transfer is uncertain. Hence it was necessary to us a two track model of the

vehicle in order to capture the locking differential transients. Another motivation to use the kinetic two track model was to capture the lateral dynamics of the vehicle when the differentials are locked. When differentials are locked, it leads to a yaw torque generation, which leads to the under-steer of the vehicle.

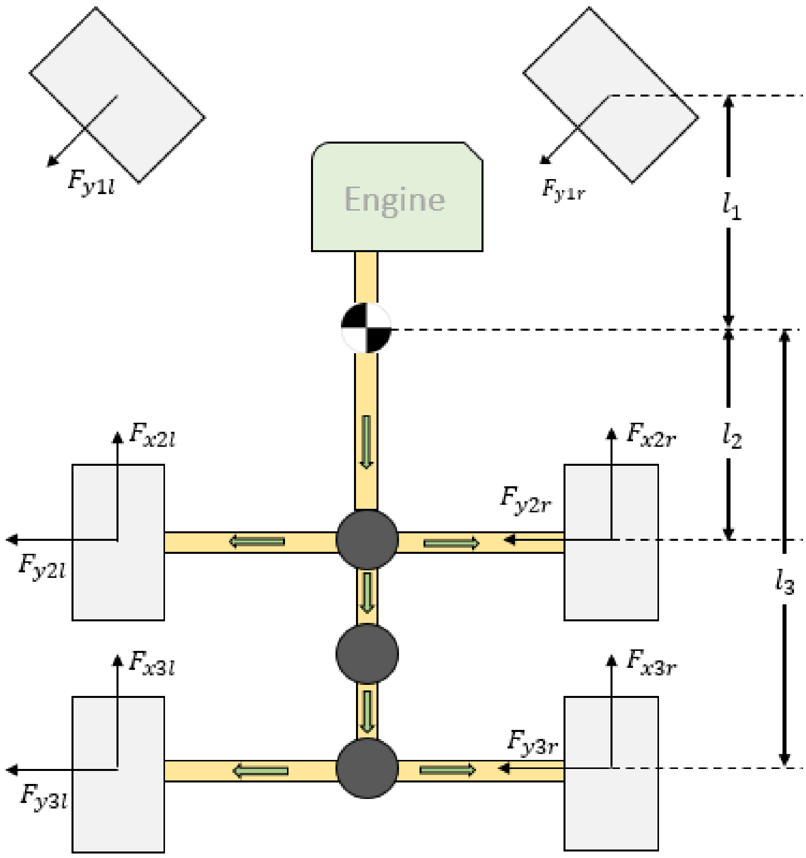

Figure 4.3: Kinetic two track model for 6x4 truck

4.2.1 Working of Prediction Model:

The prediction model works in the following steps:

Step 1: Inputs

- The model receives the road data from the environment file. The road data consists of the static road conditions (slope & curvature), the dynamic conditions (road friction) and the type of road (mud, snow, gravel, sand)
- The velocity request that is the same for the plant model
- The initial states of the vehicle
- Actuator status of the plant model (differentials locked/unlocked, normal load requests from ECS)

Step 2: Calculation of the normal loads on each axle

- With the input road data and the velocity, the road vertical velocity v_{rz} was calculated for each axle as follows:

$$v_{rz} = slope \cdot v_x \tag{4.1}$$

- Using the road vertical velocity, the chassis vertical velocity v_z is calculated and then the normal loads on each axle were calculated using spring damper equations:

$$v_{iz} = v_z - L \cdot \omega_y \tag{4.2}$$

$$\dot{F}_s = k \cdot (v_{rz} - v_{iz}) \tag{4.3}$$

$$F_s = F_s + \dot{F}_s \cdot dt \tag{4.4}$$

$$F_d = d \cdot (v_{rz} - v_{iz}) \tag{4.5}$$

$$F_z = F_s + F_d \tag{4.6}$$

where dt is the time interval to integrate states of prediction model (0.02 seconds)

Step 3: Calculation of global force requirements

- Required acceleration calculation:

$$a_{req} = \frac{v_{req} - v}{0.5} \tag{4.7}$$

- Calculation of longitudinal force request by the driver

$$F_{x,\ req} = m \cdot a_{req} \tag{4.8}$$

- Calculating the resistance forces on the vehicle

$$F_{x,\ roll} = F_z \cdot RRC \tag{4.9}$$

$$F_{x,\ grade} = m \cdot g \cdot sin(\theta) \tag{4.10}$$

- Calculating the total force required

$$F_{x,\ drive} = F_{x,\ req} + F_{x,\ roll} + F_{x,\ grade} \tag{4.11}$$

Step 4: Calculating the powertrain capabilities

- Maximum powertrain capability to produce force at velocity v

$$F_{powertrain} = \frac{P_{powertrain}}{v} \tag{4.12}$$

Step 5: Calculating the actual torque applied on the wheels

- Calculating the actual torque applied on the wheels

$$F_{x,\ total} = min(F_{x,\ drive}, \quad F_{powertrain}) \tag{4.13}$$

- Calculating the actual torque applied on the wheels

$$T_{req} = F_{x,\ total} \cdot r \tag{4.14}$$

Step 6: Calculating the tire to road force capabilities with different actuator settings

- Open differential capability for 6x4 truck

$$F_{x,open} = 4 \cdot min[(F_{z,2l} \cdot \mu_{2l}), (F_{z,2r} \cdot \mu_{2r}), (F_{z,3l} \cdot \mu_{3l}), (F_{z,3r} \cdot \mu_{3r})] \tag{4.15}$$

- Inter-axle differential locked capability for 6x4 truck

$$F_{x,IAL} = min(F_{z,2l} \cdot \mu_{2l},\ F_{z,2r} \cdot \mu_{2r}) + min(F_{z,3l} \cdot \mu_{3l}, F_{z,3r} \cdot \mu_{3r}) \tag{4.16}$$

- Inter-wheel and inter-axle differential locked together capability for 6x4 truck

$$F_{x,IWL} = F_{z,2l} \cdot \mu_{2l} + \ F_{z,2r} \cdot \mu_{2r} + F_{z,3l} \cdot \mu_{3l} + F_{z,3r} \cdot \mu_{3r} \tag{4.17}$$

Step 7: Finding the optimal actuator setting

Checking the current actuator settings of the Plant/vehicle

Set $F_{x,\text{Total}}$
if $IAL = 0$ and $IWL = 0$ **then**
$F_{x,\text{Total}} \leftarrow \min(F_{x,\text{total}}, F_{x,\text{open}})$
else
  if $IAL = 1$ and $IWL = 0$ **then**
$F_{x,\text{Total}} \leftarrow \min(F_{x,\text{total}}, F_{x,\text{IAL}})$
  else
$F_{x,\text{Total}} \leftarrow \min(F_{x,\text{total}}, F_{x,\text{IWL}})$

Calculating the states according to the actuator settings

$$a = (F_{x,f} + F_{x,total} - m \cdot g \cdot \sin\theta)/m \tag{4.18}$$

$$\dot{\omega}_y = (-(F_{x,f} + F_{x,total}) \cdot h - F_{z,f} \cdot L_{1_{CG}} + F_{z,r1} \cdot L_{2_{CG}} + F_{z,r2} \cdot L_{3_{CG}})/J_y \tag{4.19}$$

$$a_z = (F_{z,f} + F_{z,r1} + F_{z,r2} - m \cdot g \cdot \cos\theta)/m \tag{4.20}$$

Finding the required actuator setting

Set $Open\ diff.$
Set $Inter - Axle\ Diff\ Lock$
Set $Inter - Wheel\ Diff\ Lock$
if $F_{x,\text{drive}} \geq F_{x,\text{open}}$ and $F_{x,\text{drive}} \leq F_{x,\text{IAL}}$ **then**
Open diff $\leftarrow 0$
Inter-Axle Diff Lock $\leftarrow 1$
Inter-Wheel Diff Lock $\leftarrow 0$
else
    if $F_{x,\text{drive}} \geq F_{x,\text{IAL}}$ and $F_{x,\text{drive}} \leq F_{x,\text{IWL}}$ **then**
Open diff $\leftarrow 0$
Inter-Axle Diff Lock $\leftarrow 1$
Inter-Wheel Diff Lock $\leftarrow 1$
    else
        if $F_{x,\text{drive}} \leq F_{x,\text{open}}$ **then**
Open diff $\leftarrow 1$
Inter-Axle Diff Lock $\leftarrow 0$
Inter-Wheel Diff Lock $\leftarrow 0$
        else
Open diff $\leftarrow 0$
Inter-Axle Diff Lock $\leftarrow 1$
Inter-Wheel Diff Lock $\leftarrow 1$
        end if
    end if

Step 8: Updating the states for the next loop

$$v = max(0, v + a \cdot dt) \tag{4.21}$$

$$\omega_y = \omega_y + \dot{\omega}_y \cdot dt \tag{4.22}$$

$$v_z = v_z + a_z \cdot dt \tag{4.23}$$

4.3 VTM:

VTM is volvo's internal vehicle simulation software built in Matlab/Simulink.It is a complete package which includes high fidelity nonlinear mathematical vehicle models, environment model, graphical interface for visualization, and data logging. It also includes various controllers such as speed control and path follower control.

The vehicle model includes variety of tractors, rigid trucks, trailers, and semitrailers. The parameters of models are defined based on real vehicle and thus the vehicle models are highly reliable for simulation. The environment includes predefined road models whose parameters can be edited to get desired road

All vehicle models include rigid bodies such as cab, chassis and axles connected to each other through joints. The tire model used.The tires used in simulation is based on empirical Magic formula tire[Hans reference]. Vehicle models are parametric and flexible, and different combinations of tractor-semitrailer can be coupled to create suitable plant model for simulation. As it is a mathematical model and data is logged continuously, the measurement values can be used during simulation to feedback and control the plant model.

For this thesis, following plant models and controllers are used from library: 6x4 tractor,8x4 truck, engines, differentials, brakes , PAC2002 Magic formula tire models and path following controller.

The modelling and equations used in VTM's plant model is not explained due to confidentiality. A typical example of arrangement of VTM blocks used be seen in figure 4.4.

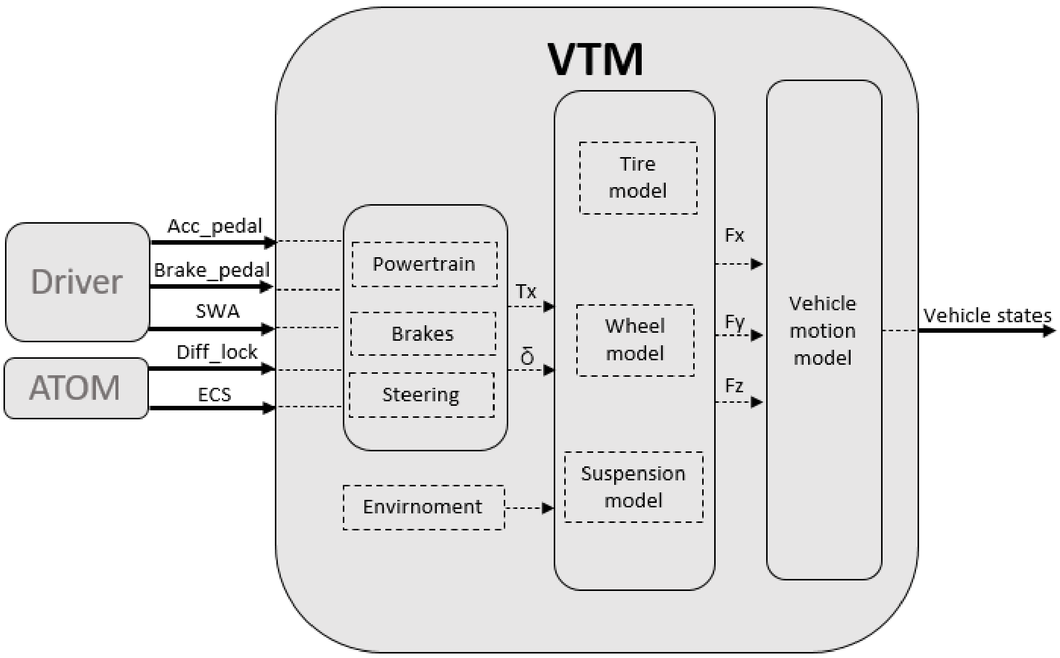

Figure 4.4: VTM plant model

5

Rapid Control Prototyping

This chapter serves as an introduction to rapid control prototyping and presents an overview of the software and hardware used to perform it. Additionally, it outlines the test setup employed in this study.

5.1 Introduction:

The commercial vehicle sector has been experiencing rapid advancements in autonomous technology. This surge is primarily driven by increasing market demand, providing safer solutions and regulatory frameworks set by governing bodies. However, a consistent challenge in this sector has been delivering technology to customers on time with the utmost efficiency and reliability. To address this challenge, Rapid Control Prototyping (RCP) has gained significant attention during the verification and validation stage. RCP serves as a methodology for quickly developing, validating and iterating functions on real-time systems. This approach aids in the early detection of faults within functions during the initial stages of development. Consequently, the time required for the entire function's development is reduced, as engineers can validate sub-functions more rapidly. Furthermore, this approach contributes to cost reduction. Late design changes can lead to high costs in adjustments and production, making it crucial to identify and rectify issues early in the development process. Additionally, RCP enhances the robustness of functions as each sub-function is validated in the early stages, resulting in a more reliable end product. This helps to validate real-time embedded systems using techniques Hardware-in-the-loop(HIL) and Vehicle-in-the-loop (VIL).

5.1.1 Hardware-In-Loop (HIL):

Hardware-in-the-loop is a testing technique that enables the interaction between a developed control system and real hardware. It accomplishes this by receiving inputs from sensors and generating simulated signals through software. HIL is vital for mimicking inputs for a virtual vehicle and its environment, allowing for the validation of the system's behavior and response in real time. Additionally, HIL provides a secure testing environment, which is especially valuable for conducting safety-critical tests safely. Covering all possible test cases in reality is challenging, whereas HIL offers the advantage of rapid execution across multiple scenarios. This ensures the quality of product, reduces cost, and enhances system robustness.

5.1.2 Vehicle-In-the-Loop (VIL):

Vehicle-in-the-Loop (VIL) is a testing technique where functions are evaluated on real vehicles within controlled test tracks, all while immersed in a virtual environment. When it comes to testing critical safety functions or progressing towards autonomous vehicles, traditional testing methods can be characterized as complex, costly, time-intensive, and often lacking in safety measures. This is where VIL steps in, offering a solution in which tests are conducted on real vehicles within a simulated environment. For instance, during a VIL test, a virtual pedestrian may be introduced into the scenario as the real vehicle is driven to assess the effectiveness of automatic emergency braking systems. This approach provides a secure testing environment for scenarios critical to safety, all without risking damage to the vehicle or its surroundings. Notably, VIL testing can be repeatedly executed to enhance performance. Typically, VIL follows Software-in-the-Loop (SIL) and Hardware-in-the-Loop (HIL) testing stages. By implementing VIL, the necessity for developing or utilizing actual test tracks and specialized testing facilities is diminished. However, it is vital that the simulation environment accurately replicates real-world scenarios and test cases.

5.1.3 Software and Hardware utilized in this thesis:

5.1.3.1 MicroAutoBox II and dSPACE ControlDesk:

MicroAutoBox II is a real-time system extensively utilized in the automotive industry for RCP and is commonly applied in both HIL and VIL simulations. The advantage of the MicroAutoBox lies in its comprehensive I/O support, accommodating standard interfaces such as CAN, LIN, FlexRay, and Ethernet. This versatile system boasts the capability to process data similar to real ECUs every 10 milliseconds. Thus, it is highly suitable for real-world testing, development, validation and optimization of control algorithms. The MicroAutoBox can be managed using dSpace ControlDesk software, serving as the crucial link between the developed TargetLink C code and the MicroAutoBox. This user-friendly tool provides a visual interface to control and fine-tune parameters, enabling the swift identification and adjustment of the Electronic Control Unit (ECU) during real-time tests. Additionally, it possesses the ability to record real-time data for later review and analysis.

5.1.3.2 CAN interface hardware and Vector CANalzyer:

The Controlled Area Network (CAN) is a standard communication protocol extensively used in the automotive industry. It facilitates data exchange and interactions among multiple Electronic Control Units (ECUs). CAN interface hardware serves as the bridge, allowing communication between external ECUs or real-time systems and the CAN network in software. This hardware replicates real-time data transmission and reception, mirroring the actual network's functionality.
CANalyzer, a tool developed by Vector Informatik, plays a pivotal role in the analysis and measurement of CAN signals and other communication networks such as LIN and Ethernet. It serves as a direct interface for communicating with ECU signals,

utilizing features like graphical visualization, signal analysis, and tracing. These capabilities are invaluable for debugging ECUs, identifying faults, and optimizing control within the CAN. In essence, CAN is a fundamental communication protocol, while CANalyzer, supported by CAN interface hardware, empowers engineers with the tools needed for thorough signal analysis and network optimization.

5.2 Test setup for ATOM controller:

In this section, steps taken to implement and test the algorithm developed on the real vehicle are explained. The implementation process involved real-world testing, including bench testing and testing on an actual vehicle.

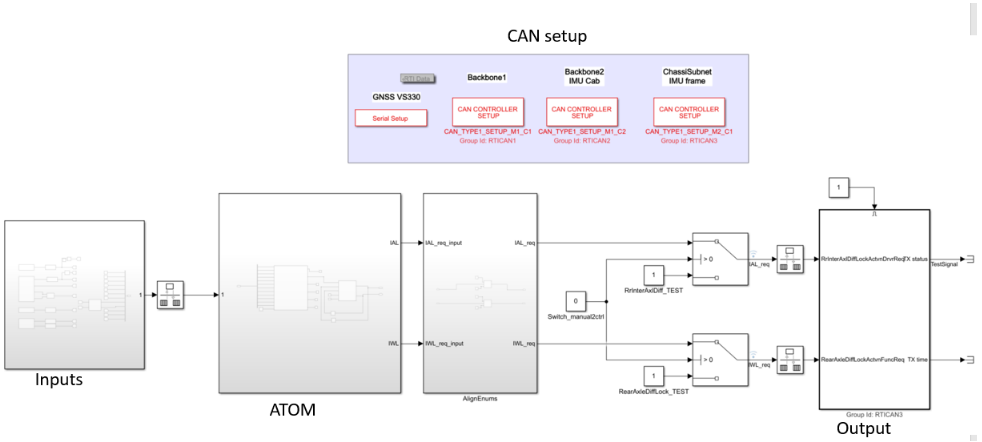

Figure 5.1: ATOM setup in Simulink

The developed ATOM algorithm was initially modeled using the Real-Time Interface (RTI) CAN Blockset in Simulink as shown in the figure 5.1 Inputs to the model were sourced from a CAN bus, which was connected to various channels of the MicroAutoBox. The setup was configured using the RTI CAN Blockset in Simulink. The left block in the figure 5.1 signifies direct model inputs, which were sourced from other CAN network buses. The inputs are as follows:

- Velocity request
- Vehicle velocity
- Distance travelled
- Vehicle pitch
- Inter-axle differential lock status
- Inter-wheel differential lock status
- Axle loads

The output signals for the differential requests were transmitted using a CAN output block. Subsequently, this model was converted into C code using TargetLink within the Simulink environment. The C code was then deployed onto the MicroAutoBox platform using the dSpace ControlDesk environment. The MicroAutoBox was connected to a computer via an Ethernet cable.

The complete setup was subsequently tested on a dedicated test rig, which included a Vehicle Master Control Unit (VMCU), the MicroAutoBox, and a CAN network

interface connected to a computer. The primary objective was to examine differential lock signals and its transmission from the VMCU to Rear chassis I/O module (RCIOM), responsible for sending requests to the differential.
In general, the operation involves a switch within a real vehicle, VMCU sends this signal to RCIOM and accordingly, the differential state is changed. But in the rig, inputs were sent from VMCU to the CAN network interface which was connected to the computer. The output from the MicroAutoBox and dSpace ControlDesk was also carefully examined to ensure it matched the expected signals by the VMCU. The CANalyzer software played a crucial role in signal analysis during this stage. The figure 5.2 shows the HIL rig setup.

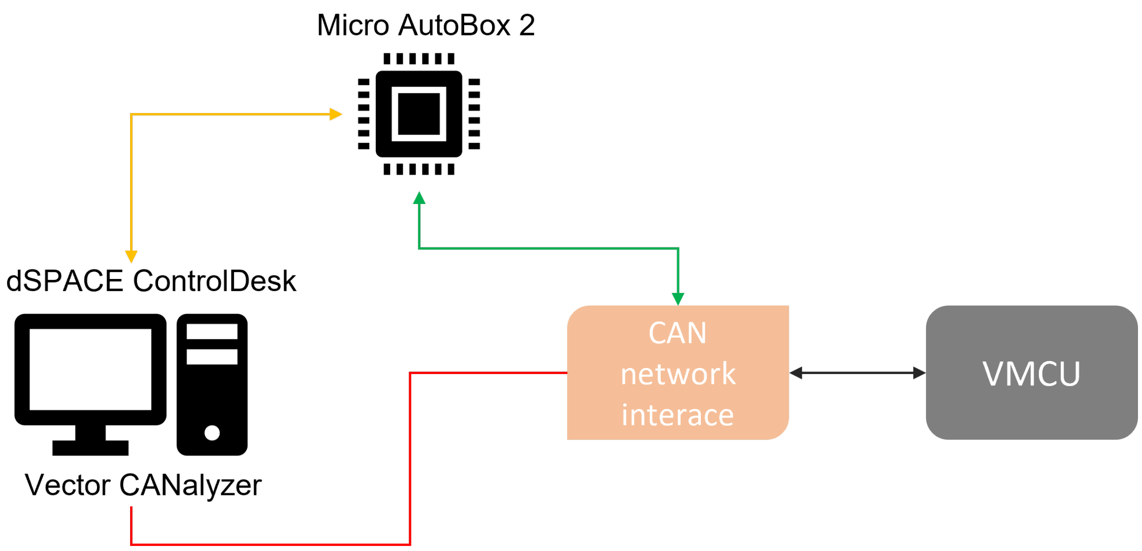

Figure 5.2: HIL rig setup

The subsequent task involved the creation of a gateway between the VMCU and the RCIOM. A gateway was established to bypass differential values from the dashboard and overwrite them with signals from the MicroAutoBox (ATOM algorithm). CAN network Chassis subnet includes differential requests. The gateway was established using a 4-channel CAN network interface and a Computer-Aided Protocol Language (CAPL) script within Vector CANalyzer. The script was designed to capture all signals from the VMCU, replacing the differential request from the MicroAutoBox and then forwarding them to RCIOM. This configuration allowed for selective signal manipulation while ensuring all other signals from the VMCU were transmitted directly. This process was critical in optimizing control over the differential system, and HIL setup was particularly advantageous in saving time and resources during the implementation phase.

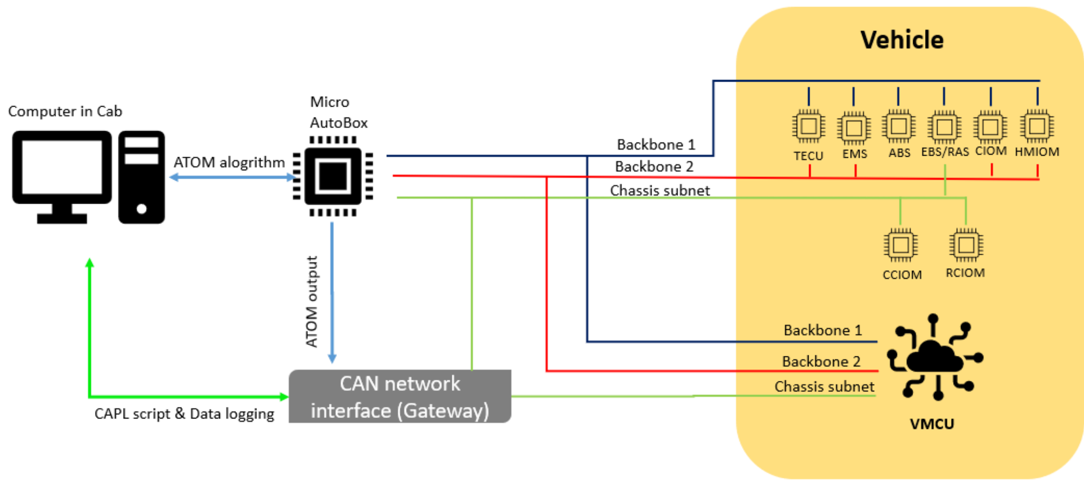

Figure 5.3: Vehicle-in-the-loop setup

Following the successful execution and gateway development, the entire setup was replicated on a real vehicle as shown in figure 5.3. Due to the unavailability of the test track and its corresponding road profile, new logic was integrated to create a virtual road within the Simulink environment. This virtual road model was seamlessly integrated with the previously developed RTI Simulink model. A critical parameter was introduced to monitor and reset the distance traveled within ControlDesk. The same test cases as previously evaluated during simulation were recreated.
During the real-world testing, a virtual 50-meter road data segment was made available to the ATOM control logic every time as input. This data was then utilized to generate differential requests, which were subsequently transmitted from the MicroAutoBox to the RCIOM. The complex setup during the real test, featuring multiple CAN networks and nodes, was effectively managed. Importantly, as the HIL setup was established initially, this phase was significantly streamlined. To replicate the same connections used in the HIL rig, a breakout harness was created. This allowed for consistent connections and a seamless transition to real-world testing. Additionally, this phase of testing proved invaluable for assessing the real-time processing capabilities of the prediction algorithm, providing insights into its performance under actual operating conditions. The error observed during the testing is explained in the chapter below.

5.2.1 Task overrun:

Task overruns were frequently observed during real-time testing with the RTI. An overrun situation arises when a task is instructed to commence its execution, but its prior instance is still ongoing and hasn't completed its calculations. Upon investigating this issue, it became evident that the root cause was the predictive algorithm, which required more time for execution than the ECU processing time allowed. The generated C code was designed to analyze signals at 10 millisecond intervals. Given that the algorithm was implemented as a Matlab function block, it retrieved inputs at 10 millisecond time steps and commenced calculations. These calculations took longer, resulting in the task overrun problem.

To address this challenge, two methods were employed. The initial approach involved code optimization, which entailed removing unnecessary code lines and utilizing commands with lower computational requirements. However, this optimization had only a limited impact on mitigating task overruns.

The second method focused on determining the algorithm's turnaround time, a process facilitated by dSpace ControlDesk. The time required for the algorithm to complete one calculation for the next 50 meters, known as the turnaround time, was established at 100 milliseconds. Consequently, a rate transition block, as depicted in the figure 5.4, was integrated to manage inputs. This adjustment allowed the function to execute calculations only every 100 milliseconds.

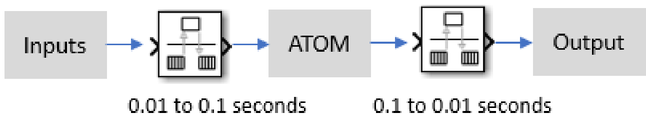

Figure 5.4: Solution for task overrun error

It was further suggested that in future implementations, the algorithm would not run at fixed intervals of 10 or 100 milliseconds. Instead, it would be triggered on-demand, rendering 100 milliseconds a more efficient computational interval for predicting data over a 50-meter range.

6

Simulation results & analysis

6.1 Introduction:

In this chapter, the results of our simulations and real-time VIL tests are presented. The format of the result graphs remains consistent across all test cases, structured in a 3x2 grid as follows:

- **Row 1, Column 1:** This graph illustrates the inter-axle differential lock request from the prediction algorithm, shown in blue as the predicted output for the next 50 meters. The actual status of the inter-axle differential lock of the vehicle is represented in green.
- **Row 2, Column 1:** In this graph, you can observe the inter-wheel differential lock request from the prediction algorithm, displayed in blue as the predicted output for the next 50 meters. The actual status of the inter-wheel differential lock of the vehicle is shown in green.
- **Row 3, Column 1:** This graph focuses on the vehicle's velocity. The predicted velocity from the prediction algorithm (in blue) for the next 50 meters is compared to the actual vehicle velocity (in green).
- **Row 1, Column 2:** This graph provides details about the road elevation for the vehicle. The road profile extends up to the next 50 meters, with a dotted black line indicating the endpoint.
- **Row 2, Column 2:** The graph depicts the predicted distance traveled for the next 50 meters, shown in blue, followed by the actual distance traveled from the start of the simulation represented in green.
- **Row 3, Column 2:** The final graph in the grid displays various force predictions. The blue curve represents Fx drive, which is the required force of the vehicle for the predicted road profile. The magenta curve, Fx open, represents the predicted open differential longitudinal force capabilities. The cyan curve, Fx IAL, represents the longitudinal force capability of the driven axle group with the inter-axle differential lock configuration, while the red curve, Fx IWL, represents the longitudinal force capability of the driven axle group with both inter-axle and inter-wheel differentials locked.

All these graphs are time-based, and the conclusion of the blue curve, which signifies the prediction, is marked as the endpoint. Additionally, a vertical red dashed line is used to indicate the vehicle's position and the start of the prediction.

6.1.1 Test cases:

1. Take off on a straight road with high friction:

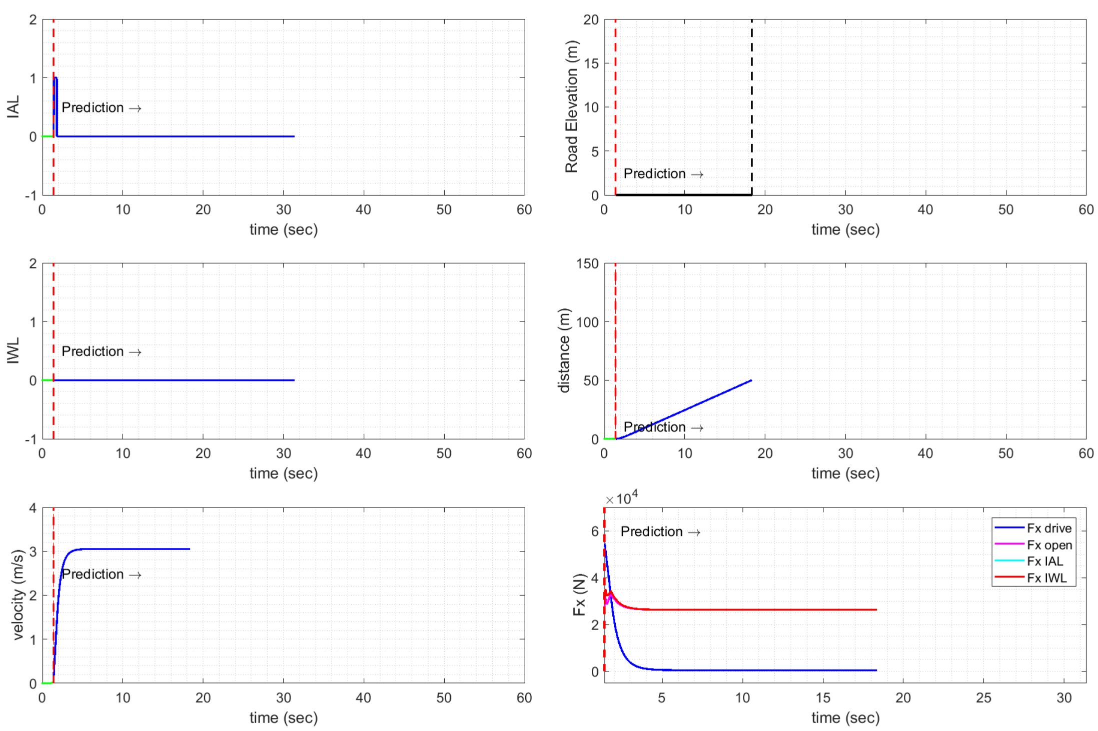

Figure 6.1: Initial take off on high friction road

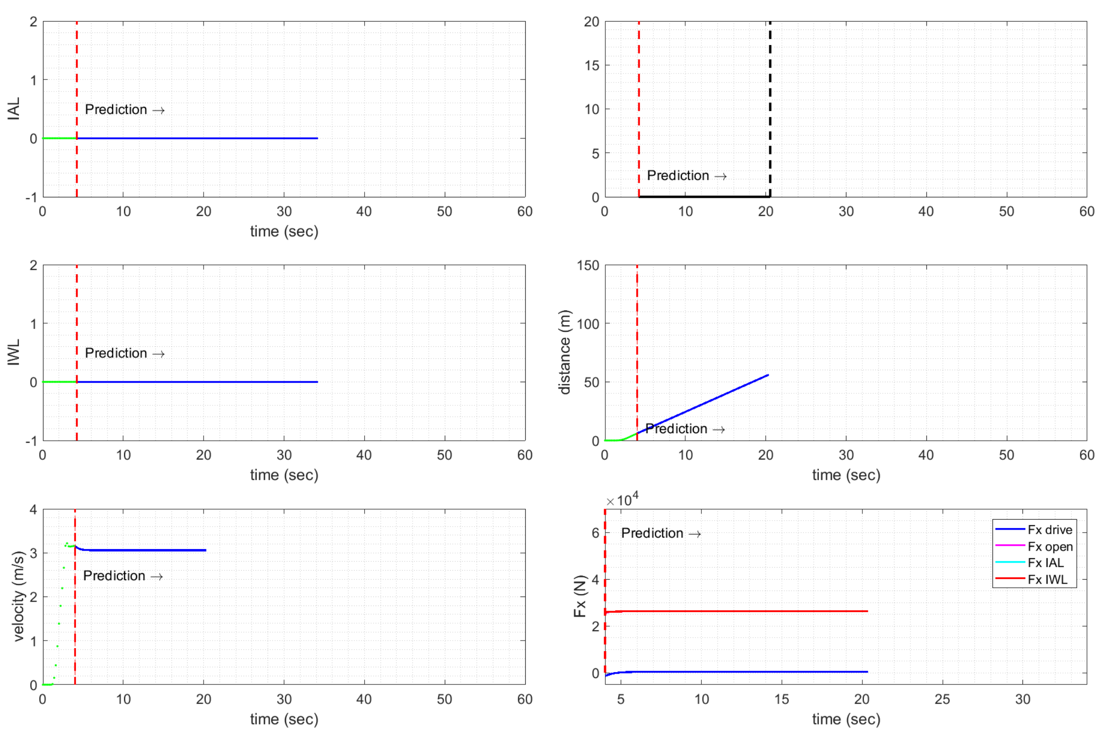

Figure 6.2: Vehicle at reference velocity on high friction road

- In this test case, referring to figure 6.1, initially the prediction model sends out a signal to lock the inter-axle differential. In the force graph in the figure 6.1, as it is a straight road with same (high) friction on both the sides of the vehicle, and the normal forces on each axle are same hence it can be seen that the maximum road wheel capabilities of both the rear axles in same. The initial required traction force is very high due to high acceleration. The model sends out a signal to lock the inter-axle differential for a very short time.
- Referring to figure 6.2, shows the response for the vehicle actuators after a few seconds of start and when the vehicle reaches its reference velocity. It can be seen in figure 6.1 that the prediction model sent out a signal to lock the inter-axle differential, but in figure 6.2, the vehicle doesn't lock the inter-axle differential. This is because the controller didn't sent out the signal to lock the inter-axle differential as it was for a very short time. In this case the reactive systems can intervene and control the wheel slip.

2. Take off on a straight road with low friction:

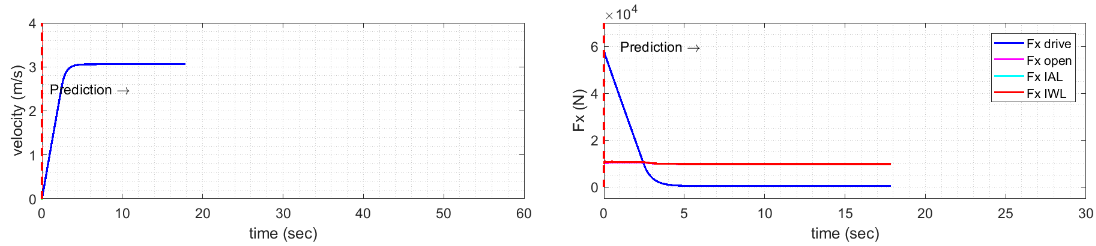

Figure 6.3: Initial take off on low friction road

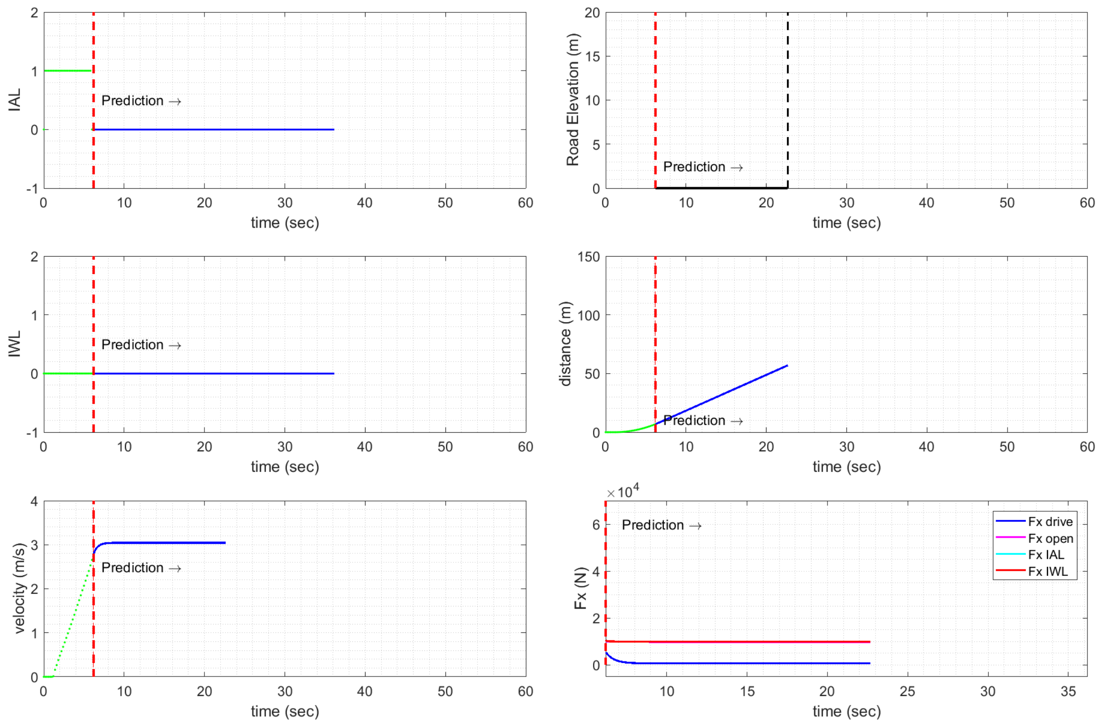

Figure 6.4: Vehicle at reference velocity on low friction road

- The figure 6.3, shows the initial response of the prediction model in this test case. It can be seen that the prediction model sends out a signal to lock the inter-axle differential in the beginning for some amount of time. In the force graph it can be seen that it is a straight road with same (low) friction on both the sides of the vehicle, and the normal forces on each axle are same hence it can be seen that the maximum road wheel capabilities of both the rear axles in same. The required drive force is higher than the open differential capabilities, hence the prediction model sends a signal to lock the inter-axle differentials.
- The figure 6.4, shows the response of the controller and the vehicle as the vehicle reaches its reference velocity. It can be seen that the vehicle has locked inter-axle differentials, and the required drive force in the force graph has dropped below the open differential capability, the prediction model sends out a signal to open all the differentials.
- In this simulation the road friction is low hence the vehicle will have a higher wheel slip which can be compensated with the reactive systems which consume excess energy and it takes more time for the vehicle to reach its reference velocity. To avoid this the prediction model locks the inter-axle differentials in advance.

3. Take off on a straight road with split friction:

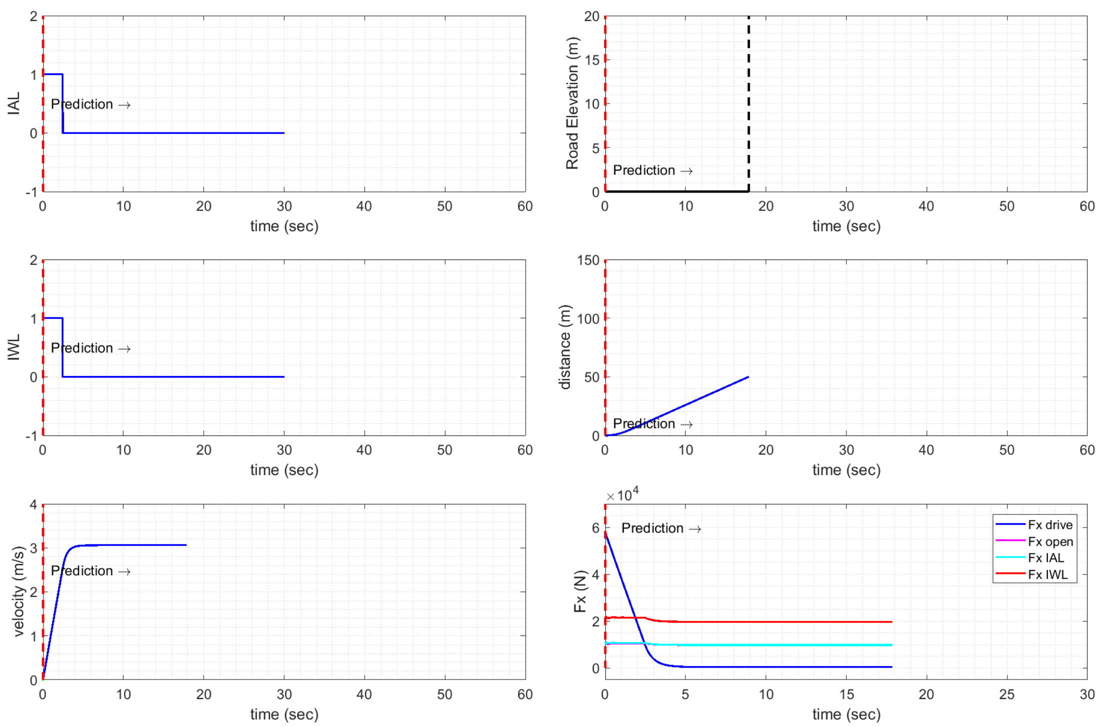

Figure 6.5: Initial take off on split friction road

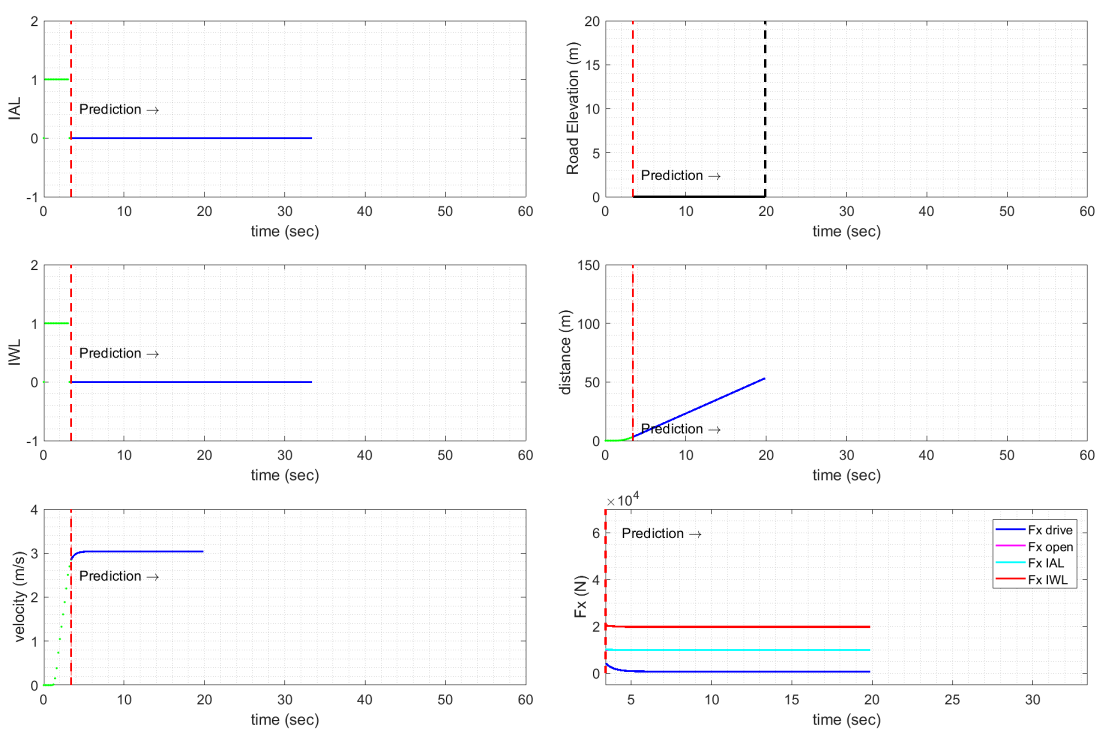

Figure 6.6: Vehicle at reference velocity on split friction road

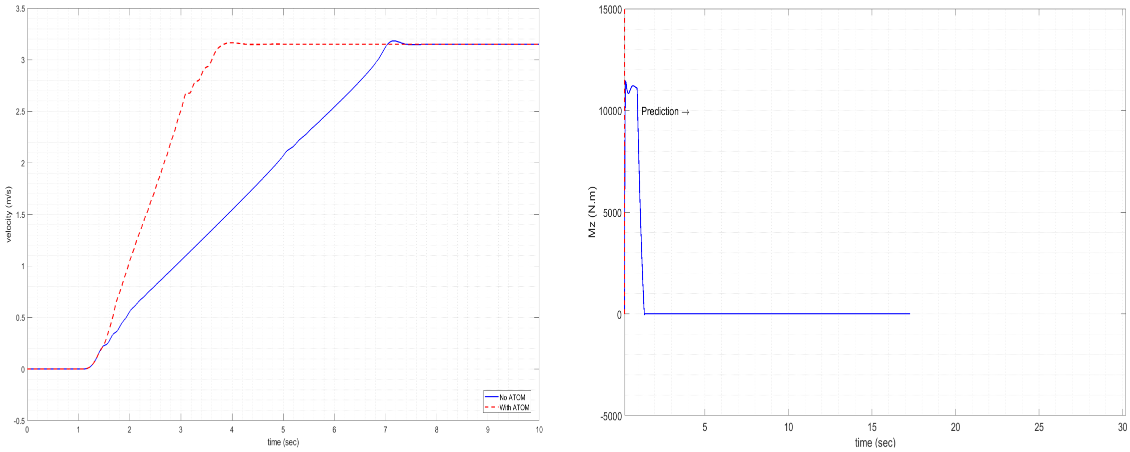

Figure 6.7: Velocity and yaw torque due to split friction on straight road

- The figure 6.5, shows the initial response of the prediction model in this test case. It can be seen that the prediction model sends out a signal to lock the inter-axle differential as well as to the inter-wheel differential in the beginning for some amount of time. In the force graph it can be seen that it is a straight road with split friction surface, and the normal forces on each axle are same, but due to split friction it can be seen that the maximum road wheel capabilities of both the rear axles in different with different actuator settings. The required drive force is higher than the open differential capabilities as well as inter-axle and inter-wheel differential lock capabilities, hence the prediction model sends a signal to lock the inter-axle as well as inter-wheel differentials.
- The figure 6.6, shows the response of the controller and the vehicle as the vehicle reaches its reference velocity. It can be seen that the vehicle has locked both the inter-axle and the inter-wheel differentials, and the required drive force in the force graph has dropped below the open differential capability, the prediction model sends out a signal to open all the differentials, when the required drive force is lower than the differential lock capabilities.
- In this simulation the road friction is split i.e. both the sides of the vehicle has different friction from each other. Hence the vehicle will have a higher wheel slip on the lower friction surface side. This will reduce the vehicle's traction capability. To avoid this the prediction model locks both the differentials in advance.
- With split friction surfaces and locked differentials the longitudinal forces on the LHS and RHS of the vehicle are different. This difference in the forces induces a yaw moment in the vehicle. In figure 6.7 on the RHS, we can see some yaw moment prediction at the start of the test as the differentials are supposed to be locked initially. The same figure 6.7 shows the difference between the speed profiles of the vehicle with predictive differential locking (dotted red curve) and normal mode (blue curve) without any traction assistance devices. It can observed that the vehicle reaches its reference velocity relatively faster when the prediction model is in action.

4. Uphill road with high friction:

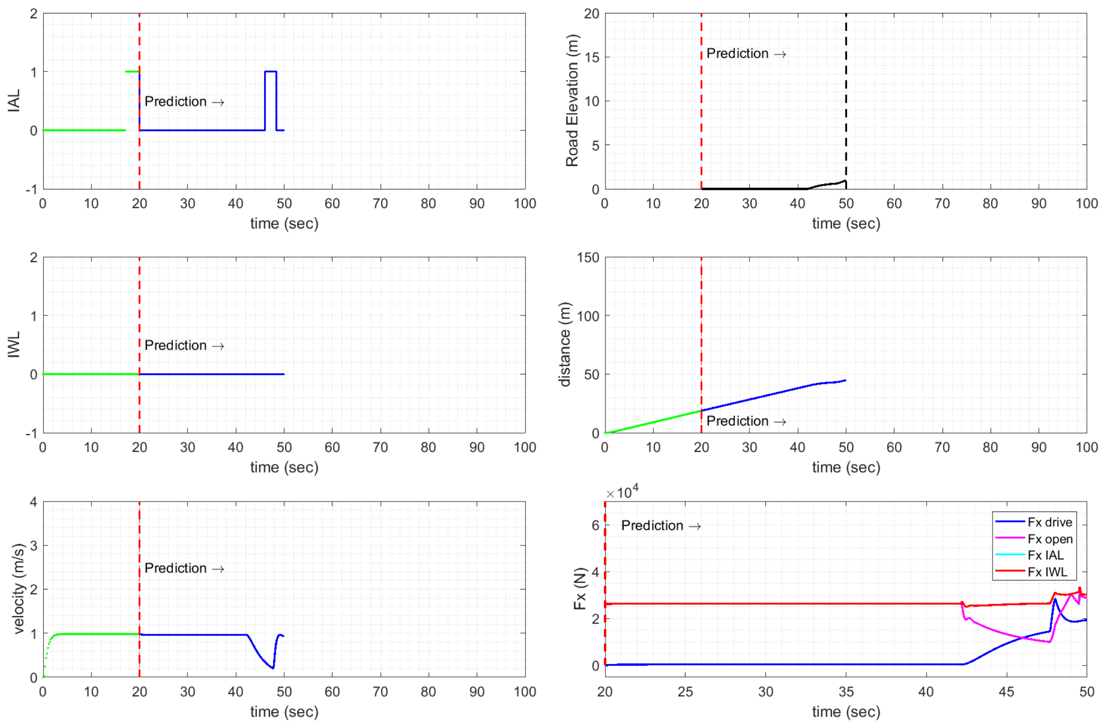

Figure 6.8: Initial uphill road with high friction

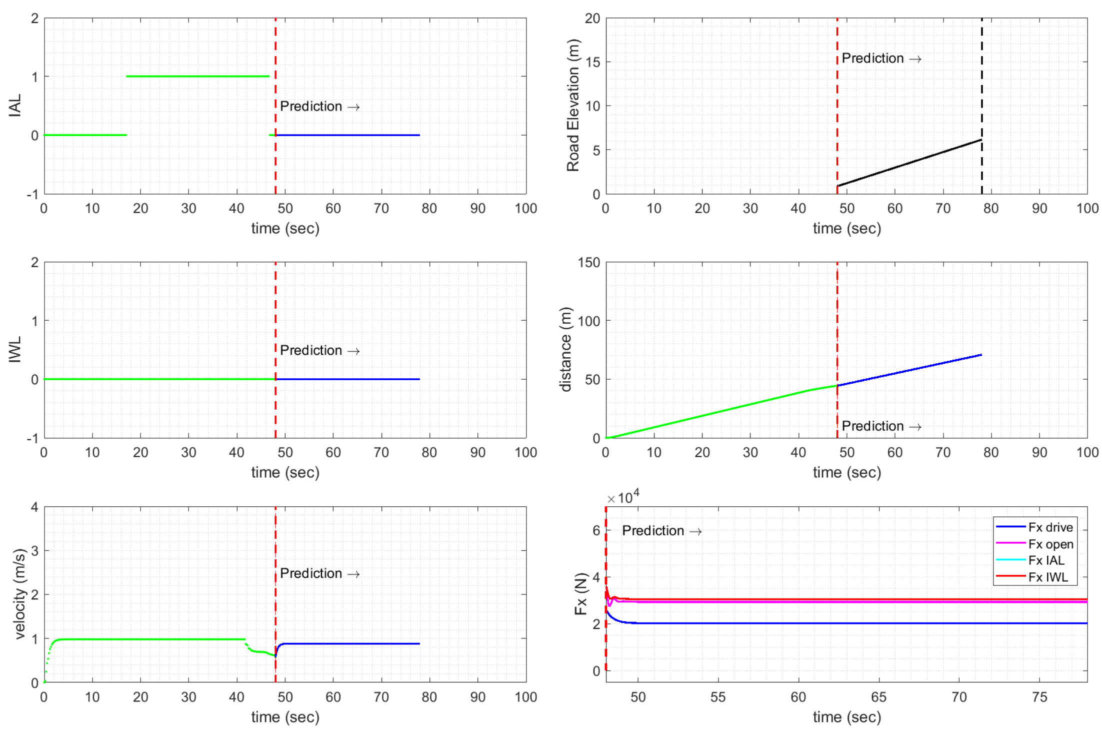

Figure 6.9: Vehicle at reference velocity on uphill road with high friction

- The fig 6.8 shows the initial response of the prediction model and the vehicle in the simulation environment for a test case of uphill with high friction road surface.
- It can be seen in all the graphs for the initial 20 seconds until where the vehicle has reached, road is flat and straight till around 40 seconds as seen in the road elevation graph. But after 42 seconds we can see there is an elevation in the road which will result in pitching of the vehicle.
- In the velocity graph it can be seen that the velocity of the vehicle will drop when it hits the road elevation. To reach the reference velocity the required drive force is increased. An increase in the required driving force is observed in the Fx graph due to the grade resistance of the road.
- At that instant where the prediction model predicts increase in the required drive force, the inter-axle differentials are locked which can be seen in IAL graph.
- In the Fx graph it can be observed that the required drive force ie above the open differential force capability but is less than the force capability of the IAL and IWL which led the prediction model to lock only inter-axle differential and not the inter-wheel differential.
- The fig 6.9 shows the final result of the test.
- In this figure it can be seen that the inter-axle differential was locked for a significantly longer time.
- It can be observed that the differential was unlocked when the model predicted that the vehicle will reach the reference velocity and the required drive force in Fx graph is less than the open differential capability of the vehicle.
- In this test case the inter-wheel differential and the onter-axle differential had same force capability due to uniform friction on both the side of the vehicle. As both the differentials had same force capability the model sent out the reponse to lock only inter-axle differential to avoid over usage of the IWL actuator.

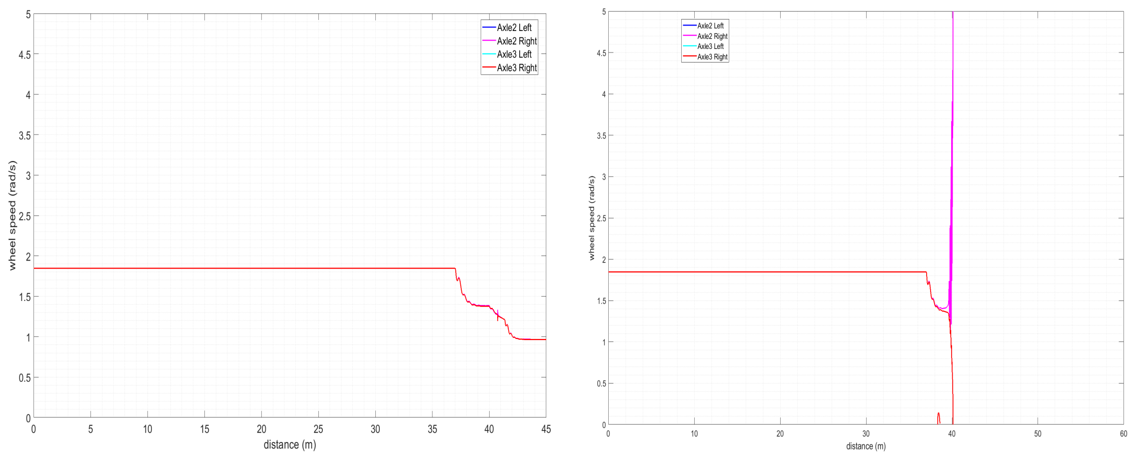

Figure 6.10: Wheel speeds of the driven axles on uphill road with high friction with and without ATOM with respect to distance

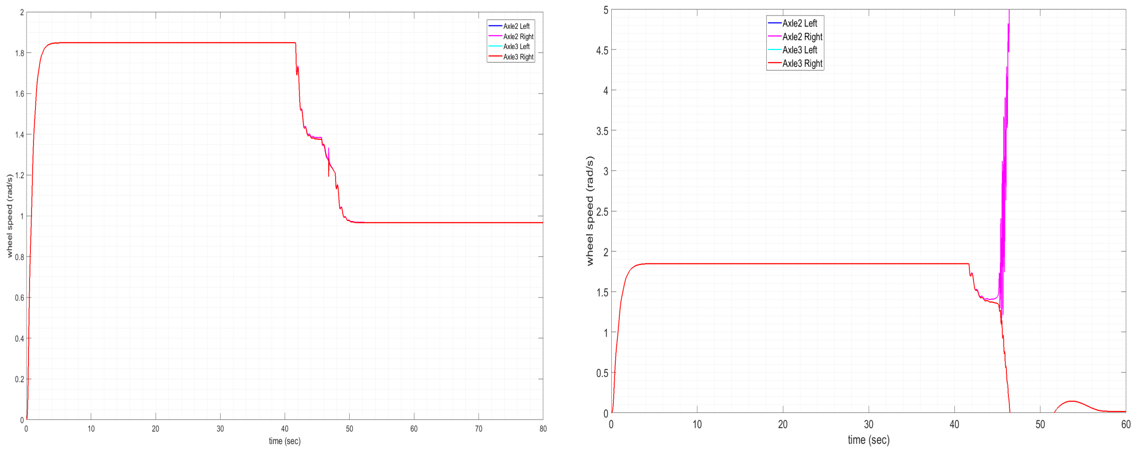

Figure 6.11: Wheel speeds of the driven axles on uphill road with high friction with and without ATOM with respect to time

5. Uphill road with low friction:

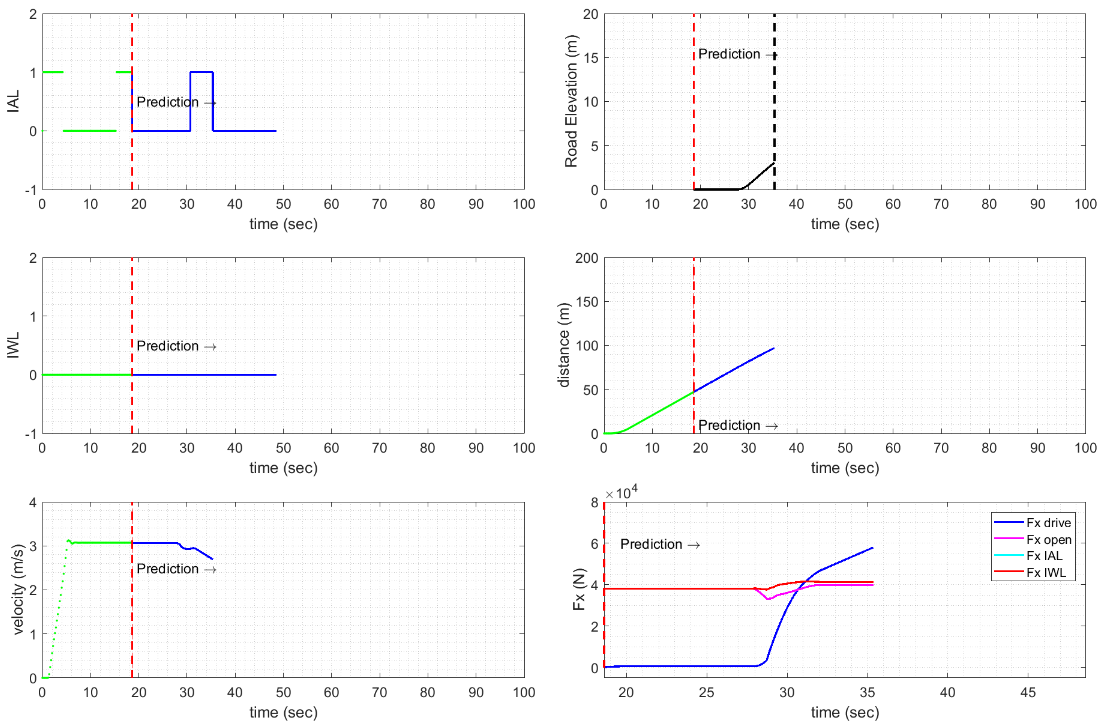

Figure 6.12: Initial uphill road with low friction

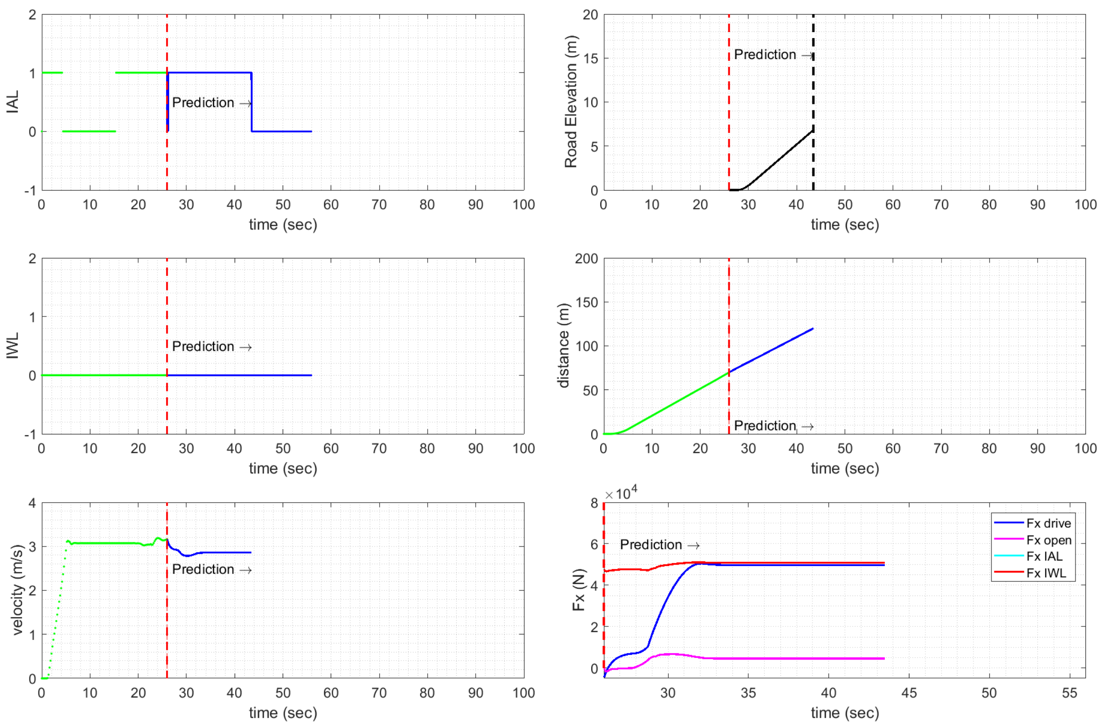

Figure 6.13: Vehicle at reference velocity on uphill road with low friction

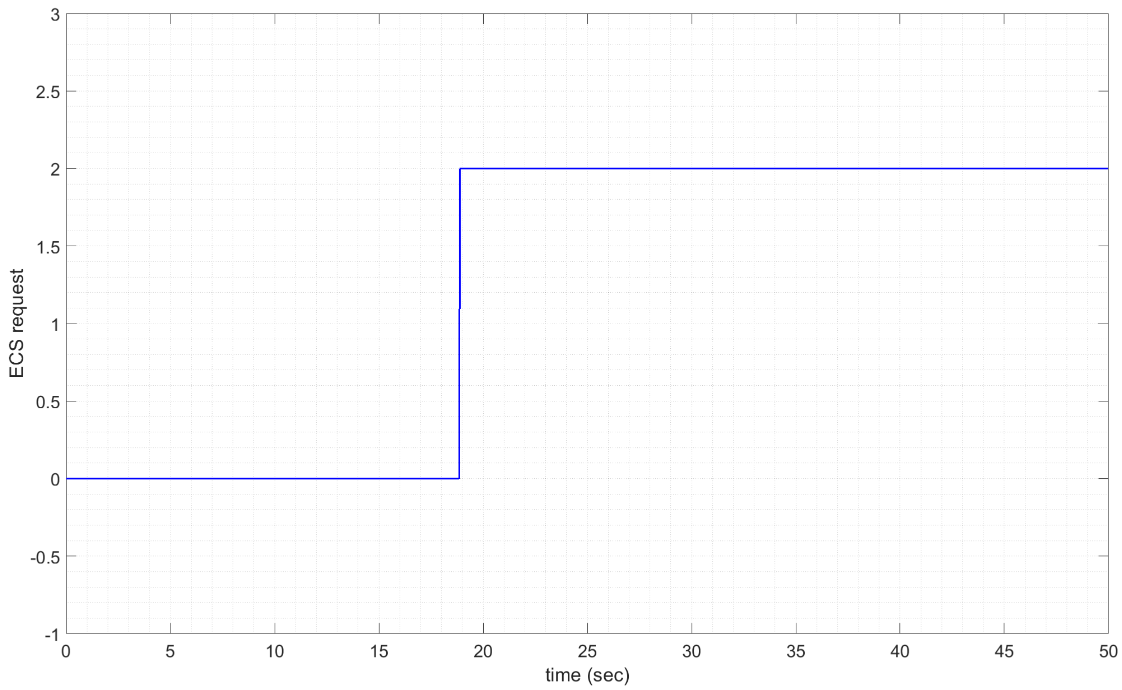

Figure 6.14: ECS request from ATOM

- The fig 6.12 shows the initial response of the prediction model and the vehicle in the simulation environment for a test case of uphill with low friction road surface.
- It can be seen that initially the vehicle has locked the inter-axle differential for a few seconds. This is due to the low friction surface. Initially when the vehicle starts due to pitching of the vehicle the normal load on the first driven axle reduces. With this load shift due to pitching and low friction surface the first driven axle loses its longitudinal force capability due to which the prediction model sends in a IAL request.
- It can be seen that the vehicle reaches the reference velocity in less than 10 seconds but the prediction models predicts that the velocity will decrease as it detects an uphill around 30 seconds in the simulation.
- It can also be observed that the required longitudinal force for the vehicle is more than the open differential force capability. Hence it sends a IAL request, which can be seen in the figure.
- It can also be observed in the force graph that the required longitudinal force is more than the IAL and IWL force capability.
- To overcome this the prediction model sends in a request for ECS to add additional normal force on the driven axles to increase the longitudinal force capability of the vehicle. This signal can be seen in fig 6.14.
- The fig 6.13 represents the vehicles response and the prediction model's response after detection of uphill in the simulation environment. It can be observed that the prediction model has sent in a IAL request and the vehicle has inter-axle differentials locked before encountering the uphill.
- A change in the longitudinal force capability of the IAL configuration can be observed in the Fx graph. This is due to the additional load added on the

driven axles using ECS.

- After all this actuator settings it can be seen that the vehicle will reach its reference velocity and climb the uphill which was not the case without the actuator settings prediction as seen in fig 6.12. Significant changes in the velocity profile and the Fx graph can be observed in both the figures.
- All these actuator settings are done before the vehicle encounters the uphill.

6. Uphill road with split friction:

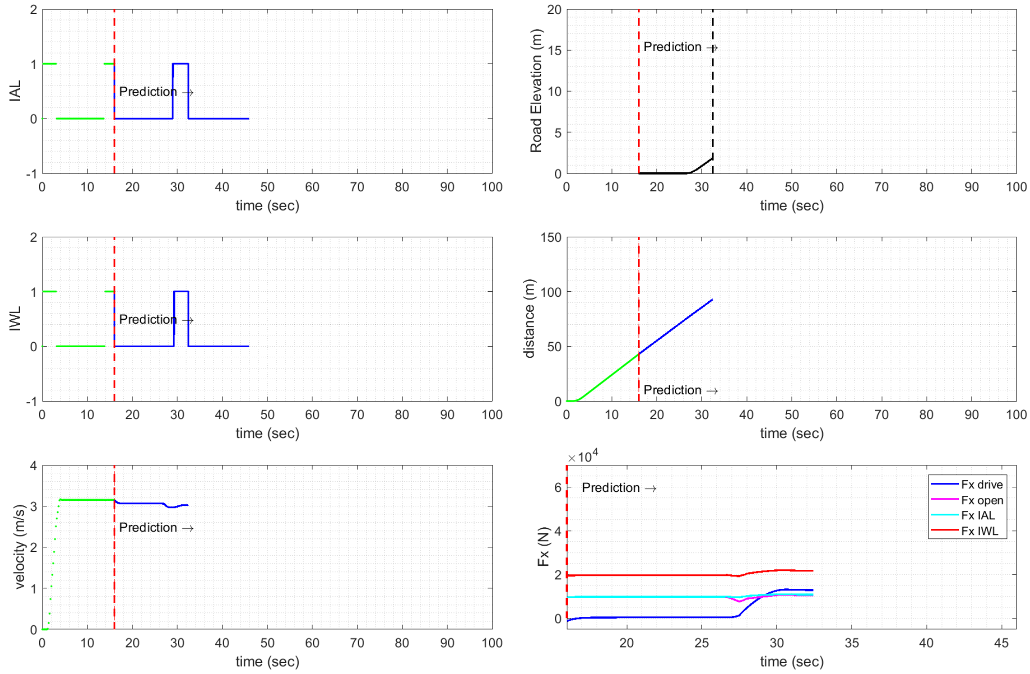

Figure 6.15: Locking of differentials due to split friction road

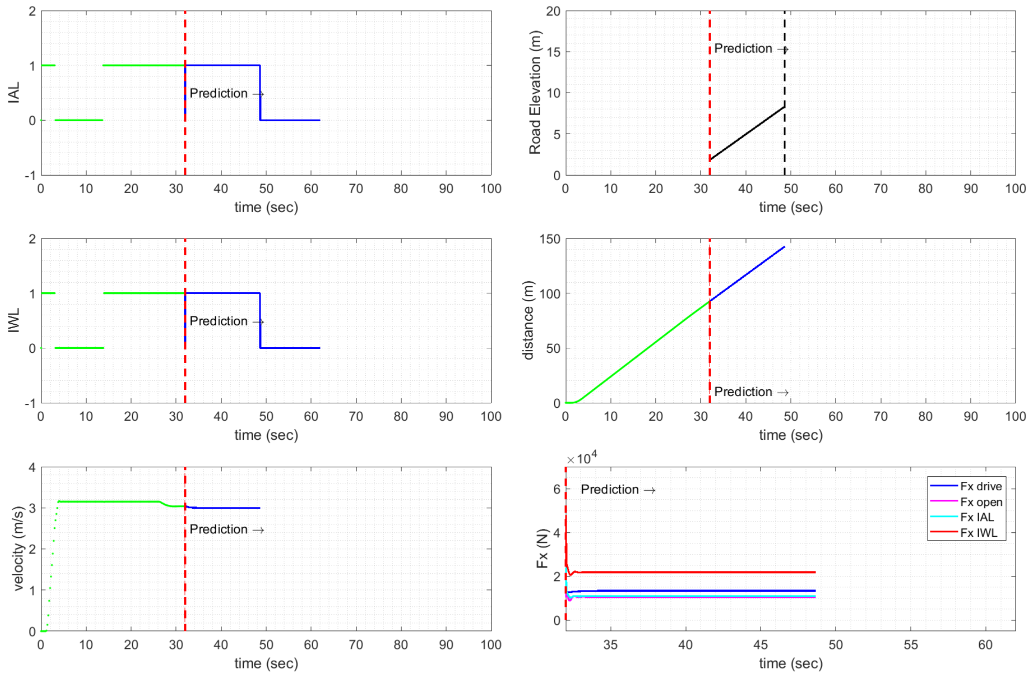

Figure 6.16: Locked IWL in uphill with split friction road

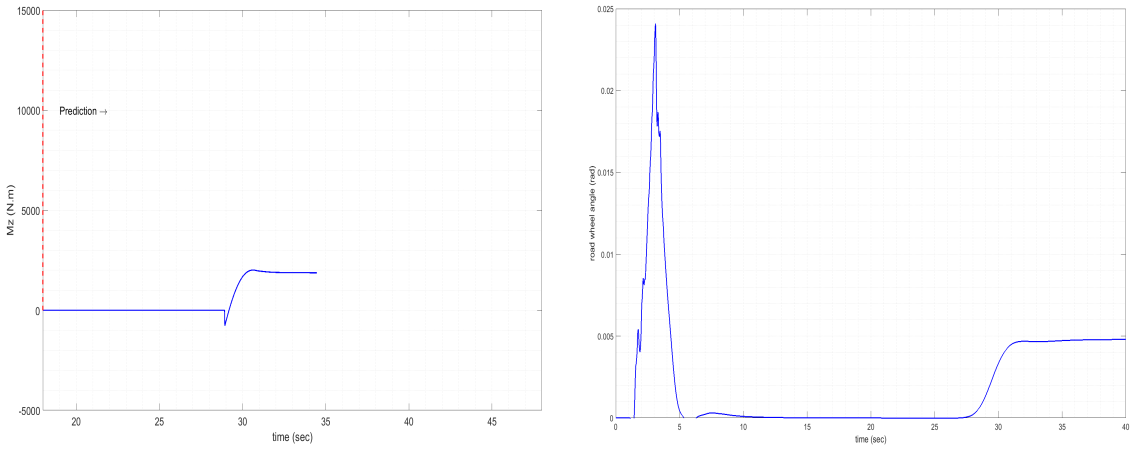

Figure 6.17: Yaw torque generation due to split friction surface and the steering compensation required

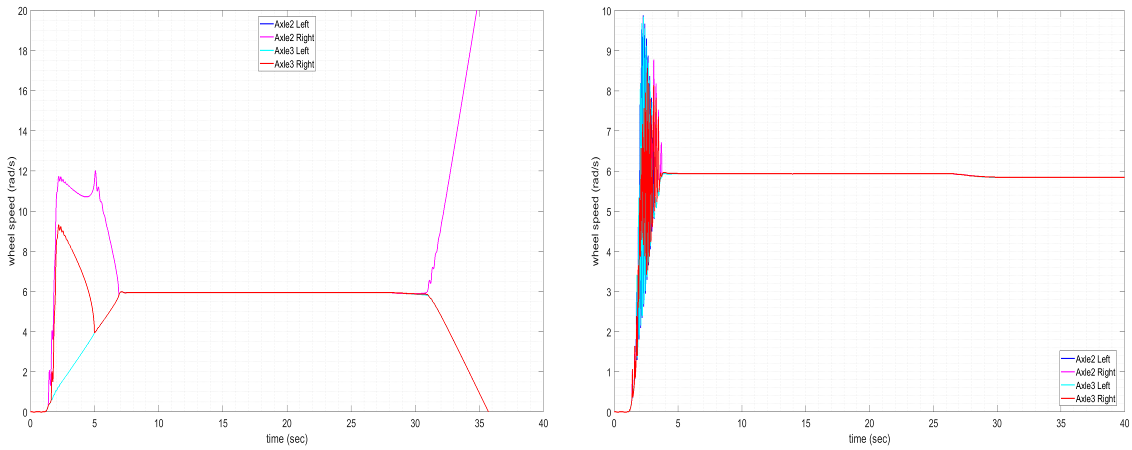

Figure 6.18: Wheel speeds of the driven axles on uphill road with split friction with and without ATOM with respect to time

- The figures 6.15, 6.16, 6.17 and 6.18 represent the results for the simulation of the test case uphill with split friction surface.
- In fig 6.15 it can be observed that the IWL request and the IAL request is on for the initial few seconds. Due to the split friction surface the longitudinal force capability of driven axle group will be limited with the low friction side. Having open differential configuration would result in wheel slips. To avoid this the prediction model locked the inter-axle and inter-wheel differentials.
- In the same figure it can be observed that the the prediction model detects uphill in the road and the required longitudinal force is predicted. It can also be observed

6.1.2 VIL test results:

A virtual road was designed to replicate the test scenarios conducted in simulations. Initially, various types of roads were generated, including those with low friction, high friction, and split mu surfaces. Subsequently, a final road was constructed, consisting of 100 meters of low friction, followed by a 13% uphill slope with split mu friction properties. This particular road was devised to evaluate the performance of both IAL and IWL differentials on an actual truck. Efforts were made to maintain the vehicle's speed close to the reference velocity of 3 m/s. Figure 6.24 show the velocity of real vehicle vs time during the test. It is important to note that the real truck was physically driven on a high friction, level road, but virtual road conditions were employed as inputs to the algorithm in order to trigger differential behavior. All the results below are for the final road setup.

- Figure 6.19 show the take off event on low friction. As observed in simulations results, the global force required (Fx drive) is higher than the capabilites of the differential locks and thus, the interaxle is locked for first 12 seconds.
- After 12 seconds, when the vehicle has achieved its reference speed, the inter-axle differential is unlocked as the Fx drive just needs to overcome rolling resistance. Figure 6.21 explains the prediction of force request for unlocking stage. The figure also includes how much distance is covered by the vehicle and uphill when the prediction is calculated. The actual request and status of IAL can be observed in figure 6.20.

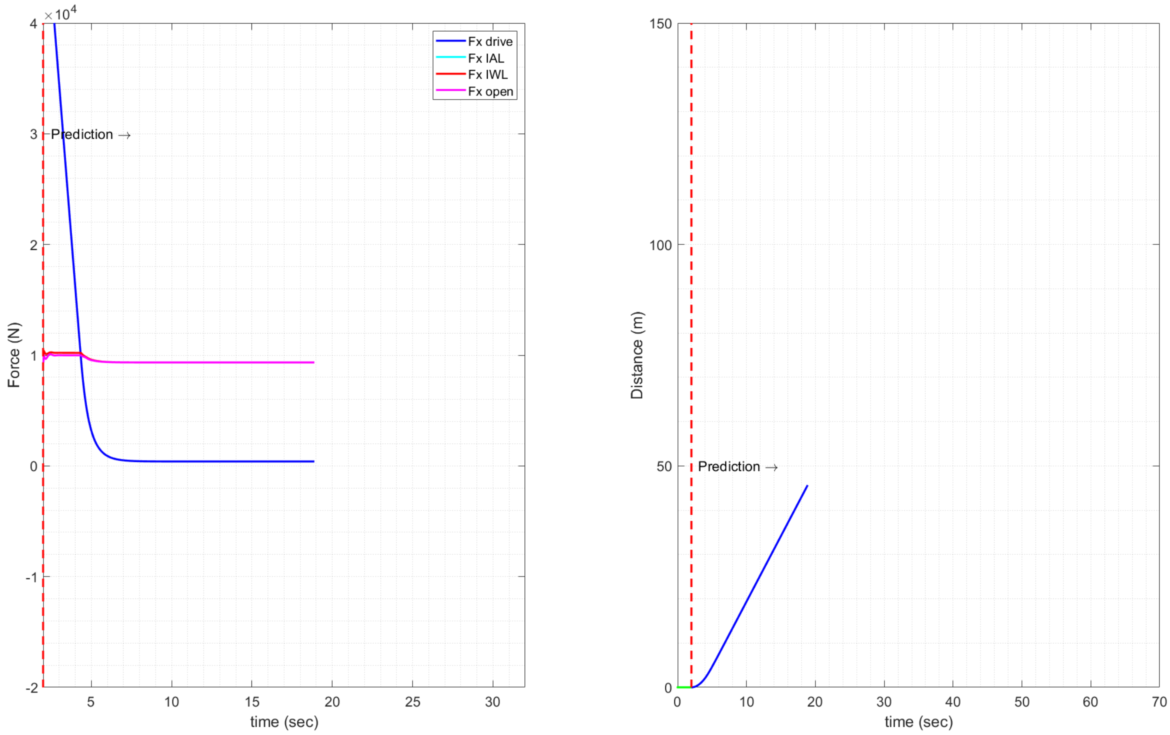

Figure 6.19: Initial take off on low friction straight road

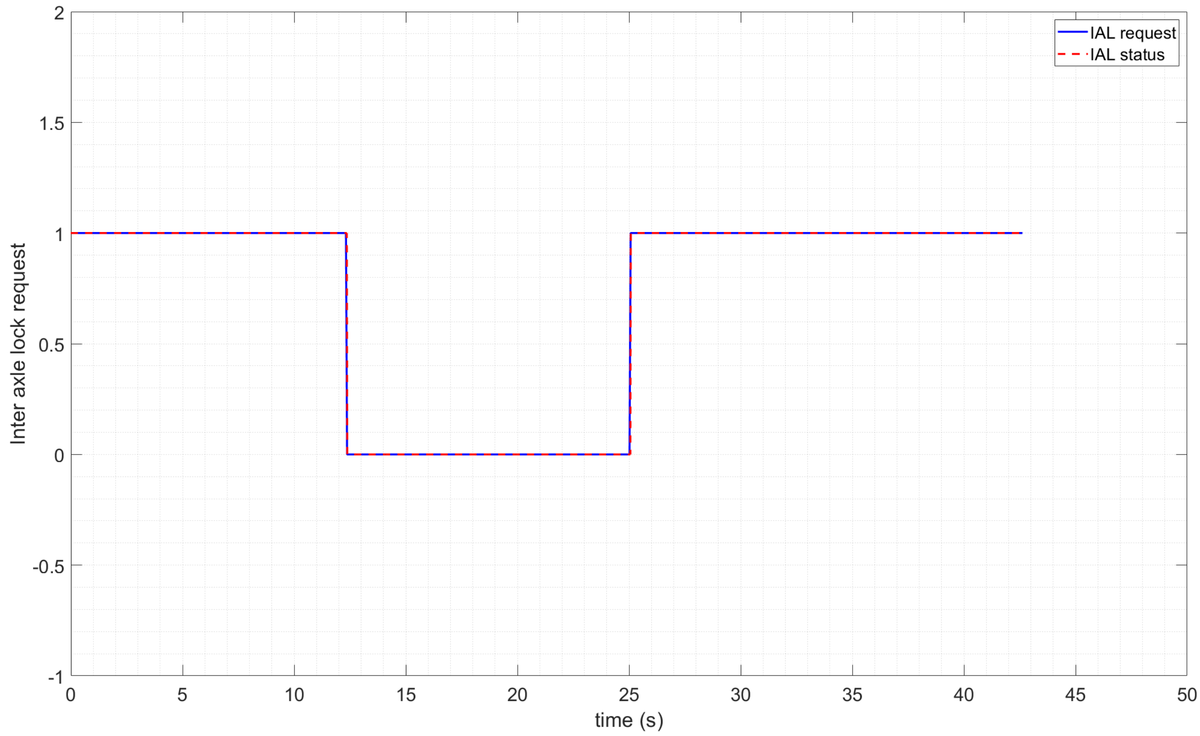

Figure 6.20: Locking of inter-axle differential due to low friction road

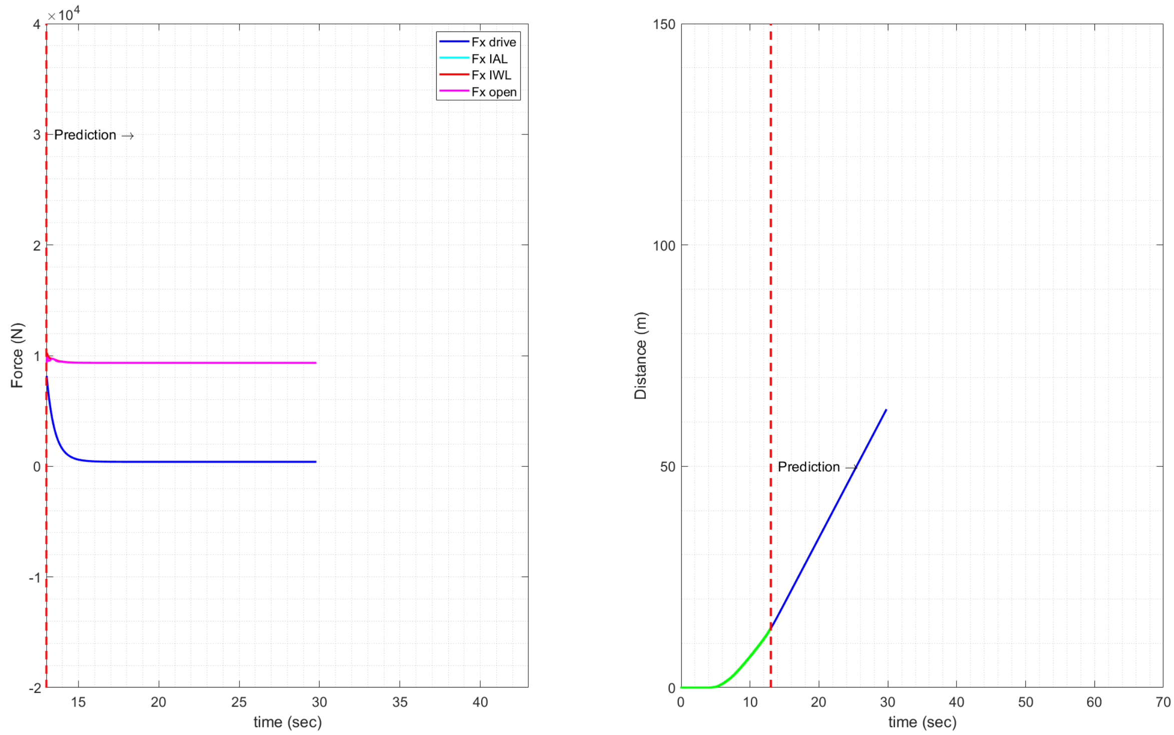

Figure 6.21: Vehicle at reference velocity on low friction surface

- Figure 6.22 explains the locking of both the differential. As explained above in the test case, the road has an uphill with split mu after 100 seconds. The distance graphs depicts that the prediction is for upcoming slope till 110 meters. This can be seen in force diagram as well. After 40 seconds, the Fx drive starts to rise as the vehicle needs to overcome uphill slope. Also, as it is split mu, the IWL and IAL capabilities are different. Thus the both the differentials are locked when the vehicle reaches a distance of approximately 60 meters, i.e way before than the slope is encountered. Thus, the prediction algorithm validates with the simulation results. Figure 6.23 shows IWL vs time (seconds). The differential request is sent at 25 seconds which is when the vehicle has travelled around 60 meters. The differentials were locked until the end of measurement as the slope was continued in virtual road.

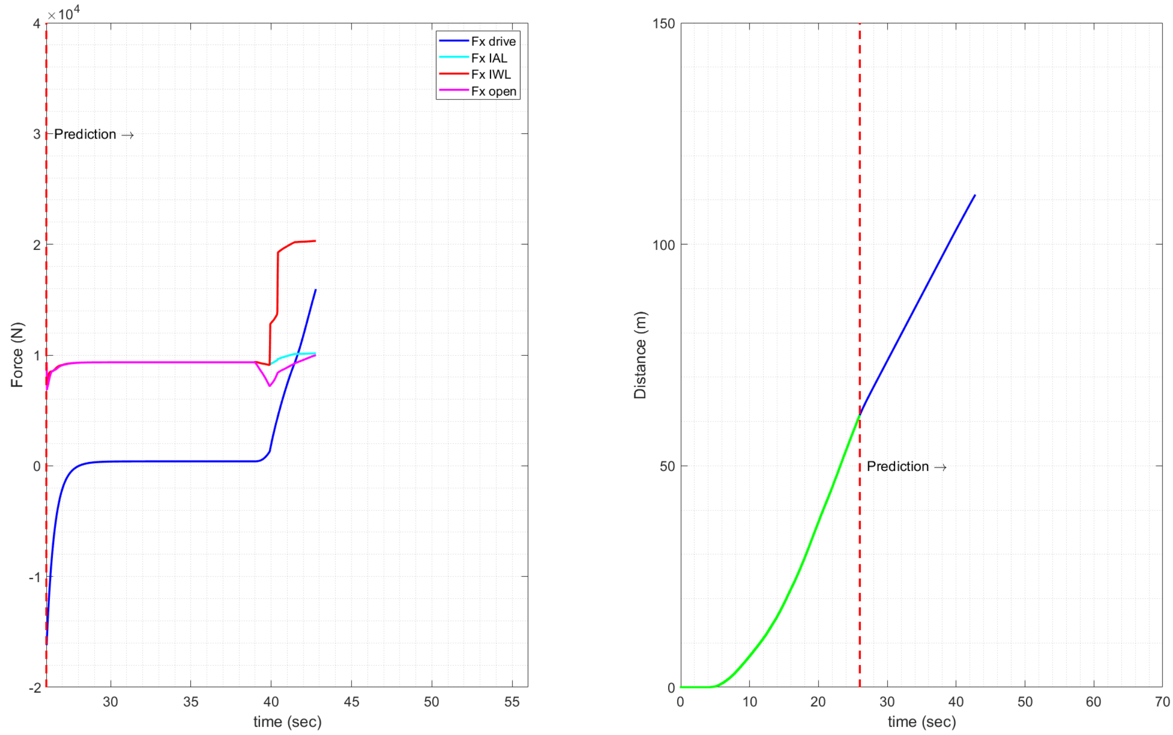

Figure 6.22: Change in drive force request due to uphill and split friction

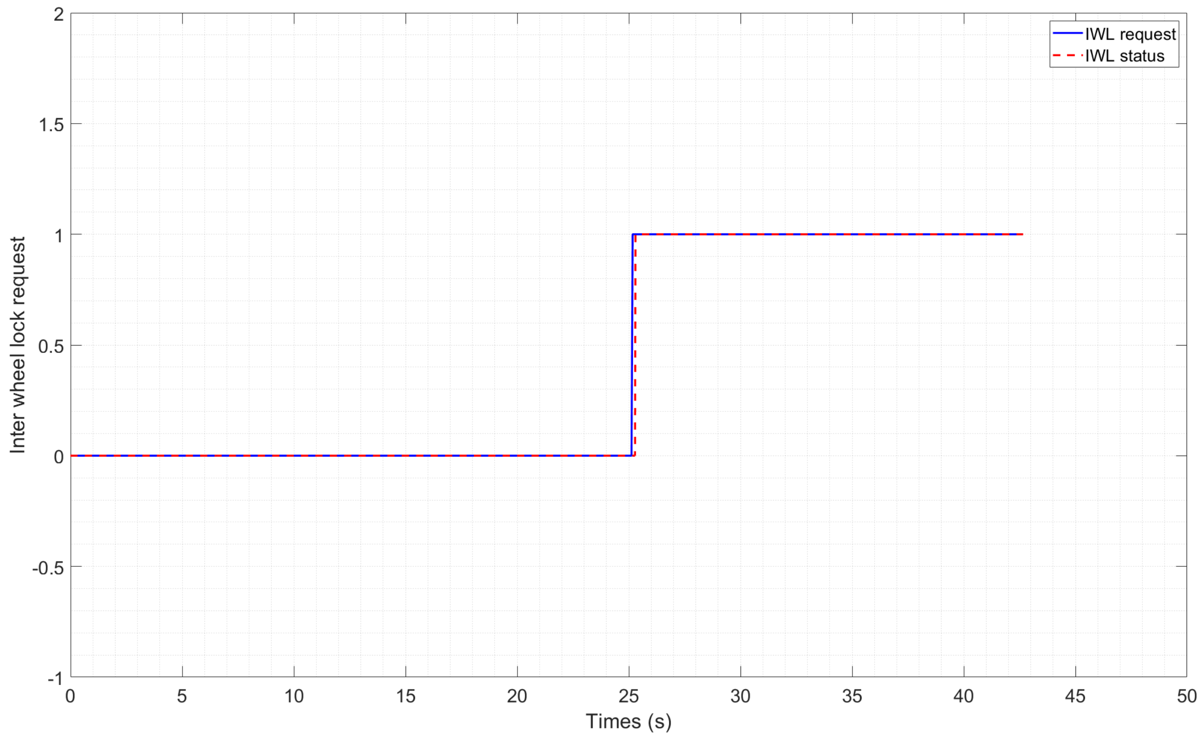

Figure 6.23: Locking of inter-wheel differential on the split friction surface

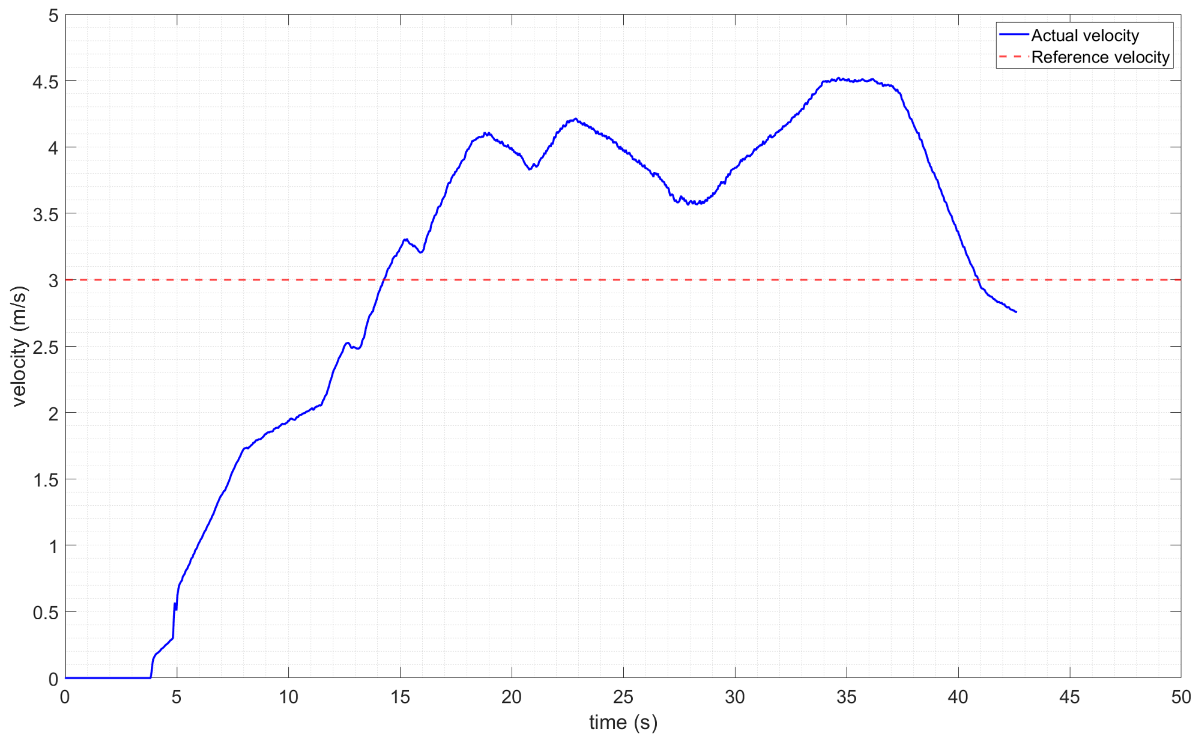

Figure 6.24: Velocity of the vehicle

7
Conclusion

The main objective of thesis was to develop and verify algorithm for automatic control allocation of differential locks and electronically controlled air suspension to maximize traction based on predicted road data information. The objective is fairly achieved by predicting capabilities based on simple vehicle dynamics mathematical model running in a ‘for loop’ for the entire prediction horizon. The result depicts that the prediction of lateral and traction capabilities of differential locks and ECS over a long-time horizon is possible using this method and can be implemented on real control unit.

The best actuator setting for different road terrains requires understanding of properties of road surface deformation when vehicle passes over it. Modelling of such phenomenon was difficult and thus not developed. To tackle this objective, values of rolling resistance and friction were tuned to get desired properties of mud, gravel, and snow.

Effect on locked differential on traction and steering helped understand important concepts such as longitudinal and lateral scrubbing on wheels and axles. The function to calculate steering angle correction due to locked differential was developed and simulated in VTM. The algorithm had small errors when compared to actual steering angle and it was due to the fact that nonlinear tire and combined tire slip was not considered. Although the traction control system was not involved during simulation and testing, the control allocation logic was developed such that overuse of differential lock and/or traction control by brake is minimized. The simulation results showed that the axle load distribution or lifting one of the driven axles has no significant benefits on traction capabilities, compared to a vehicle that has liftable dead axle. Thus, initially the algorithm was only developed for lifting one driven axle for 6x4 and further the scope was extended to 8x4 tractor to have better understanding and control logic for axle load distribution. The concept of Performance matrix is proposed to solve the usage of ECS and differential locks for special test case i.e., Uphill in turn, but it was not implemented in simulation due to time constraints.

MicroAutobox II was used to implement and verify the prediction control allocation method in real time. HIL and VIL testing was carried out and the response was analyzed. It took less than 0.1 seconds in real time to predict capabilities and make decision over 50 meters of prediction horizon. Thus, the simplicity of the vehicle dynamics model used for prediction helped to succeed this method. There are many improvements that can be further worked on to increase the accuracy of predictions and to get better decisions. Those are explained in future scope

8

Future Work

Below is the list of future research and development directions that hold the potential to advance control allocation for such actuators and improve vehicle dynamics modeling and control.

- Developing technology for prediction road data: The existing work included creation of virtual road and performing VIL. This can improvised by replacing it with actual road data from camera, GPS and other sensors.
- Utilizing Modelica for Vehicle Mathematical Modeling: The existing prediction model developed in MATLAB introduced complexity to the modeling process. Modelica offers an advantageous alternative by enabling the solution of nonlinear equations without the need for explicit conversion. This facilitates the development of more intricate vehicle dynamics models, incorporating elements such as nonlinear tire models and steering angles. Additionally, the conversion of Modelica models to Functional Mock-up Units (FMUs) allows for seamless simulation in other software environments.
- Optimizing Differential Delay and Locking Assistance: The delay between the request and the status of the differential is intricate and requires further investigation and testing for a comprehensive understanding. This complexity can be integrated into the control allocation process. Moreover, the implementation of a differential locking assistance function can significantly reduce the response time. This function can selectively apply braking to specific wheels, synchronizing shaft speeds and expediting locking and unlocking. Further enhancements can be made to the Electronic Control System (ECS) performance matrix by introducing additional combinations into the controller, possibly through methodologies like dynamic programming.
- Machine Learning Integration: Investigating the incorporation of machine learning techniques to further refine control allocation, can be an option worth considering.
- Rolling Resistance and Friction Estimation: Developing models for rolling resistance and fricti on estimation will further optimize the results from the prediction control.
- Study of Lateral and Longitudinal Wheel Scrub Effects: The effect of locked differentials and multiple axles on truck dynamics, particularly the lateral and longitudinal wheel scrub effects needs to be investigated as this will enhance the prediction of lateral and longitudinal capabilities.
- Extension of Control Allocation with ECS Roll Torque Request: The allocation can be further extended by incorporating ECS roll torque requests to alter

loads on the left and right sides of the vehicle. This will require an in-depth study of the ECS system.

- Parallel Execution of Multiple Models: Implementing a smart parallel execution approach for multiple models with various combinations can be an option. However, this might result in higher computational time.

Bibliography

[1] Bengt Jacobson (2022) Compendium in Vehicle Motion Engineering, Vehicle Dynamics Group, Division Vehicle and Autonomous Systems, Department of Mechanics and Maritime Sciences, Chalmers University of Technology.

[2] Meet Dabhi Karthik Ramanan Vaidyanathan (2017) Automation and synchronization of traction assistance devices to improve traction and steer-ability of a construction truck. Master Thesis report at KTH Royal Institute of Technology

[3] Björn Källstrand (2016) Control Allocation for Vehicle Motion Control: Maximizing Traction and Steering Capabilities Under Different Road Conditions. Master Thesis at Chalmers University of Technology.

[4] Patrik Hopkins and L. Daniel Metz (1994) Oversteer/Understeer Characteristics of a Locked Differential, University of Illinois at Urbana-Champaign.

[5] Martin Holmgren Olof Bengtsson (2013) Rear axle steering for heavy duty trucks, evaluating and improvement of maximum steering angle of tag axles for Volvo tridem trucks. Bachelor thesis at Chalmers University of Technology.

[6] Amato Tito*, Frendo Francesco, Guiggiani (2004) Massimo Handling behavious of vehicles with locked differential systems. Department of Mechanical, Nuclear and Production Engineering, University of Pisa, Italy.

[7] Mats Jonasson (2019) Vehicle dynamics models for normal force estimation.

A

Appendix 1

A.1 Longitudinal wheel scrubbing: Effect of locked differential on lateral dynamics

Locking the inter-axle differential has a minimal impact on vehicle handling compared to locking the inter-wheel differential. To assess the effects of a locked inter-wheel differential or having all differentials locked on the steering, the following methods and assumptions are employed.
Assumptions: Linear tire properties in lateral and longitudinal direction, Longitudinal force only on driven axles and no braking on any wheel, Small lateral forces, Low-speed and steady-state cornering, Small angle approximation.

The longitudinal force acting on each wheel can be described by the equations below:

$$F_{x,ij} = C_{x,ij} \cdot s_{x,ij} \tag{A.1}$$

$$C_{x,ij} = CC_{x,ij} \cdot F_{z,ij} \tag{A.2}$$

where, i = 2 or 3 (driven axles), j = left or right wheel (refer figure 4.3)
The longitudinal slip on each wheel is determined by:

$$s_{x,ij} = \frac{r \cdot \omega_{ij} - v_{x,ij}}{r \cdot \omega_{ij}} \tag{A.3}$$

When all differentials are locked, resulting in equal wheel speeds:

$$\omega_{2l} = \omega_{2r} = \omega_{3l} = \omega_{3r} \tag{A.4}$$

The longitudinal velocity of the inner wheel can be approximated as:

$$v_{x,2l} = v_{x,3l} = v_x - \frac{T}{2} \cdot \omega_z \tag{A.5}$$

Where the yaw rate ω_z for low-speed steady-state cornering can be assumed as:

$$\omega_z = \frac{v_x}{R} \tag{A.6}$$

Conversely, the longitudinal velocity of the outer wheels is given by:

$$v_{x,2r} = v_{x,3r} = v_x + \frac{T}{2} \cdot \omega_z \tag{A.7}$$

The total propulsion force on the wheels is the sum of the longitudinal forces on each driven wheel:

$$F_{x,total} = \sum(F_{x,ij}) \tag{A.8}$$

These equations can be solved for $F_{x,ij}$ with known values of $F_{x,total}$, v_x, R, $F_{z,ij}$, $CC_{x,ij}$, r, and T. The result of this analysis reveals the longitudinal scrub force generated as the wheels are compelled to rotate at the same speed during a turn. Solving the equations leads to the conclusion that this results in an additional yaw torque moment in the opposite direction of the turn, causing the vehicle to understeer. However, it should be noted that this approach is only valid for low-speed steady-state cornering and tire slip in linear region. The Yaw torque due to locked differential can be calculated as:

$$M_z = ((F_{x,2l} + F_{x,3l}) - (F_{x,2l} + F_{x,3l})) \cdot \frac{T}{2} \tag{A.9}$$

Because of the intricate dynamics associated with locked differentials, this approach was used as an approximation to calculate lateral capabilities for test cases such as roundabouts and uphill with turns.

Figures A.1 and A.2 illustrate a comparison of a vehicle's road wheel angle while maneuvering through a curve with all-locked differentials. The simulations were conducted at a low speed of 3 m/s, with varying road curvature radii (12 and 20 m). These graphs reveal that both the prediction models exhibit some degree of error as compared to high fidelity VTM model. After doing further simulations, it was observed that the error starts to decrease as the radius of curvature is increased

Given that the thesis primarily emphasizes traction, the prediction model with a smaller margin of error was employed to calculate lateral capabilities and make decisions regarding the necessity of unlocking the differentials.

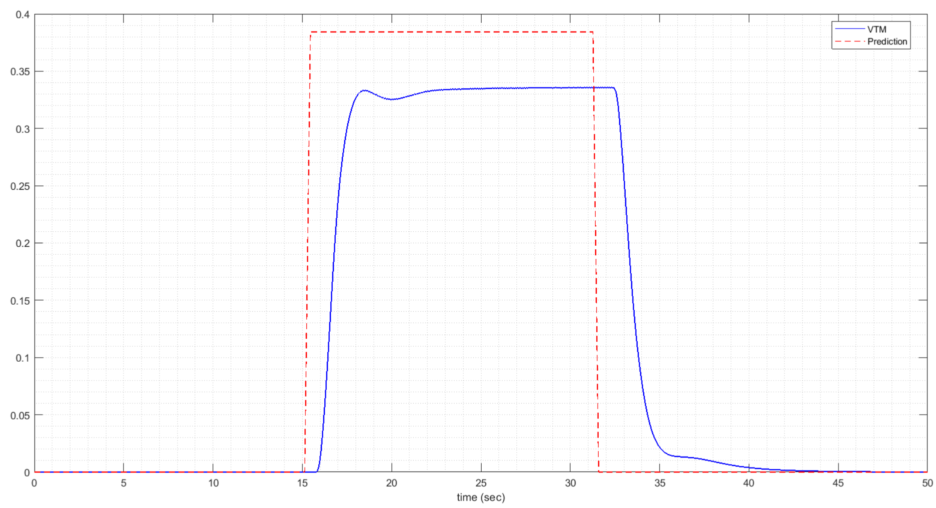

Figure A.1: Road wheel angle (rad) vs time comparison of VTM and prediction model for 12 m curve radius

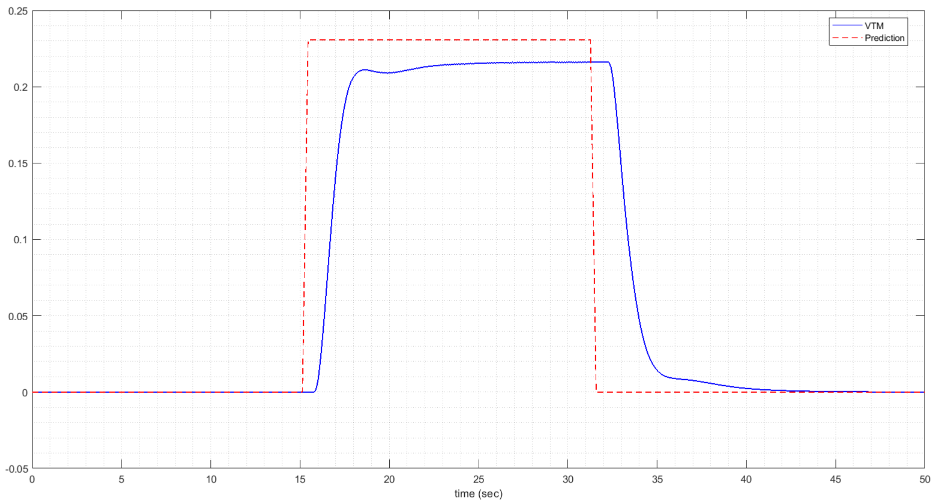

Figure A.2: Road wheel angle (rad) vs time comparison of VTM and prediction model for 20 m curve radius

DEPARTMENT OF SOME SUBJECT OR TECHNOLOGY
CHALMERS UNIVERSITY OF TECHNOLOGY
Gothenburg, Sweden
www.chalmers.se

CHALMERS
UNIVERSITY OF TECHNOLOGY